Zeeman-Type Magneto-Optical Studies of Interband Transitions in Semiconductors

E. Burstein,* G. S. Picus, R. F. Wallis, and F. Blatt†

United States Naval Research Laboratory, Washington, D. C.

(Received July 31, 1958)

In the presence of a magnetic field the quasi-continuous levels of simple energy bands are coalesced into one-dimensional sub-bands and the "time reversal" degeneracy of the levels is split. The energy levels are characterized by the quantum numbers: $\hbar k_H$, the crystal momentum along the magnetic field direction; l, the Landau magnetic quantum number; and M, the component of the total angular momentum along the magnetic field which is characteristic of the atomic states in the tight-binding limit. In the case of degenerate valence bands, the effect of a magnetic field is complicated by degeneracy effects and the levels in a magnetic field are characterized by two or more pairs of (l,M) values. The selection rules, polarization effects, and the character of the absorption spectra for interband transitions in the presence of a magnetic field are discussed and illustrated by experimental data for Ge and InSb. A discussion of practical and experimental considerations of Zeeman-type interband magneto-optical effects is also presented.

1. INTRODUCTION

ZEEMAN-TYPE experiments, which involve the effect of a magnetic field on absorption or emission spectra, have long been useful in the study of the energy levels of atomic and molecular systems. Early in 1956 such experiments were initiated on solids at this Laboratory, beginning with the observation of the intrinsic absorption of InSb in a magnetic field. These first experiments were carried out with relatively thick specimens and therefore involved the long-wavelength tail of the absorption edge. They showed that the magnetic field caused the absorption edge to shift to higher photon energies.[1]

The shift of the absorption edge corresponds to an increase in the optical band gap with magnetic field and is consistent with the theory that in a magnetic field the energy levels in an allowed energy band are coalesced into highly degenerate "one-dimensional sub-bands." The energy separation between a given sub-band in the valence band and a given sub-band in the conduction band increases with magnetic field; consequently the optical band gap increases with magnetic field. These findings were confirmed by the Lincoln Laboratory group which also extended the experiments to higher magnetic fields and to InAs.[2]

On the basis of the simple theory, it was believed that transitions between successive pairs of magnetic sub-bands in the valence and conduction bands should lead to additional structure in the intrinsic absorption. Accordingly the interband magneto-optical (IMO) experiments on InSb at the Naval Research Laboratory (NRL) were extended to thinner sections, and several prominent absorption peaks were found in fields as low as 15 000 gauss at room temperature.[3] The Lincoln Laboratory group, which had initiated experiments on

germanium in order to clarify the nature of nonlinear gap shifts with magnetic field observed in InSb and InAs, independently observed similar structure in the direct transition spectrum of germanium.[4] Since then the NRL group has carried out typical transverse and longitudinal Zeeman-type measurements at room temperature on the direct transition spectrum of germanium, using plane polarized radiation for the transverse measurements and circularly polarized radiation for the longitudinal measurements.[5] The Lincoln Laboratory group has extended its room-temperature measurements to InSb and InAs and has more recently carried out low-temperature measurements using plane polarized radiation.[6]

This paper has three purposes. The first is to discuss the physics underlying the effect of an external magnetic field on optical interband transitions. These effects, as manifested in absorption spectra, are referred to as Zeeman-type interband magneto-optical effects and are designated simply as the IMO effect. The second purpose of the paper is to report the NRL data for the room-temperature experiments on the direct transitions in germanium using polarized light and their interpretation in terms of the Luttinger and Kohn theory of the effect of magnetic field on the energy bands involved. The third purpose is to discuss practical considerations involved in carrying out Zeeman magneto-optical experiments.

2. GENERAL CONSIDERATIONS

A. Energy Levels in Simple Energy Bands

Let us first consider a semiconductor whose valence and conduction bands are "simple"; i.e., the bands are nondegenerate, have their extrema at $\mathbf{k}=0$, and the dependence of energy on crystal momentum, $\hbar\mathbf{k}$, is

* Present address: Department of Physics, University of Pennsylvania, Philadelphia, Pennsylvania.

† Permanent address: Physics Department, Michigan State University, East Lansing, Michigan.

[1] Burstein, Picus, Gebbie, and Blatt, Phys. Rev. **103**, 826 (1956).

[2] Zwerdling, Keyes, Foner, Kolm, and Lax, Phys. Rev. **104**, 1805 (1956).

[3] E. Burstein and G. S. Picus, Phys. Rev. **105**, 1123 (1957).

[4] S. Zwerdling and B. Lax, Phys. Rev. **106**, 51 (1957).

[5] Burstein, Picus, Wallis, and Blatt, "Magneto-optic Studies of Energy Band Structure in Semiconductors" in "A Decade of Basic and Applied Science in the Navy," Department of the Navy (March, 1957).

[6] Zwerdling, Lax, and Roth, Phys. Rev. **108**, 1402 (1957); Zwerdling, Roth, and Lax, Phys. Rev. **109**, 2207 (1958).

spherically symmetric and quadratic. With no magnetic field, the valence band and conduction band energy levels are given by

$$\epsilon_v(\mathbf{k}) = \epsilon_v - \frac{\hbar^2}{2m_v{}^*}(k_x{}^2 + k_y{}^2 + k_z{}^2), \qquad (1a)$$

$$\epsilon_c(\mathbf{k}) = \epsilon_c + \frac{\hbar^2}{2m_c{}^*}(k_x{}^2 + k_y{}^2 + k_z{}^2). \qquad (1b)$$

The subscripts v and c refer to the valence and conduction bands; ϵ_v and ϵ_c are the energies at the band edges; m^* is the effective mass of the carriers; $\hbar k_x$, $\hbar k_y$, and $\hbar k_z$ are the components of the crystal momentum of the carriers along the x, y, and z directions. The energy gap is $\epsilon_{G0} = \epsilon_c - \epsilon_v$. Bands for which the energy eigenvalues show a quasi-continuous dependence on each of the three components of crystal momentum are referred to as three-dimensional bands. For "simple" three-dimensional bands, the density of states, i.e., the number of states per unit volume per unit energy interval, has the form

$$N^{(3)}(\epsilon) = 4\pi(2m^*/h^2)^{\frac{3}{2}} |\epsilon - \epsilon_0|^{\frac{1}{2}}, \qquad (2)$$

where ϵ_0 is the energy at the band edge.

In the presence of a magnetic field,[7] the energies of the carriers become quantized in the plane perpendicular to the magnetic field but remain quasi-continuous in the direction of the field, thus forming a series of "one-dimensional sub-bands" (Fig. 1). The energies of the levels in the sub-bands—neglecting spin—can be written as the sum of two terms: one representing the quasi-continuous dependence of energy on the component of the crystal momentum along the direction of the magnetic field; and the other, which has the same form as

Fig. 1. Energy bands for a simple semiconductor for $H=0$ and for $H>0$.

[7] F. Seitz, *Modern Theory of Solids* (McGraw-Hill Book Company, Inc., New York, 1940), pp. 583–590.

the discrete energy levels of an harmonic oscillator, representing the quantized orbital motion of the electrons about the magnetic field direction as axis. For a magnetic field applied along the z direction, the energy levels of the charge carriers are given by

$$\epsilon_v(k_z, l_v) = \epsilon_v - \hbar\omega_{0v}(l_v + \tfrac{1}{2}) - \hbar^2 k_z{}^2/2m_v{}^*, \qquad (3)$$

$$\epsilon_c(k_z, l_c) = \epsilon_c + \hbar\omega_{0c}(l_c + \tfrac{1}{2}) + \hbar^2 k_z{}^2/2m_c{}^*, \qquad (4)$$

where l, the Landau magnetic quantum number, is a positive integer or zero and $\omega_0 = eH/m^*c$ is the circular cyclotron resonance frequency. The energy separation between successive magnetic sub-bands is $\hbar\omega_0$.

The minimum of the lowest sub-band of the conduction band occurs at an energy $\frac{1}{2}\hbar\omega_{0c}$ above the energy band minimum in zero field, and the maximum of the highest sub-band in the valence band occurs at an energy $\frac{1}{2}\hbar\omega_{0v}$ below the valence band maximum in zero field, thus increasing the band gap by $\frac{1}{2}\hbar(\omega_{0c} + \omega_{0v})$ (Fig. 1).

Each energy eigenvalue specified by Eq. (3) or (4) corresponds to a large number of degenerate states which differ from one another in the value of a third quantum number not appearing in the energy expressions. The degeneracy per unit area of the sample transverse to the magnetic field is given by $s/2\pi$ where $s = eH/\hbar c$. The size of the free carrier orbits in the xy plane, as determined by their root mean square radius, is given by[8]

$$r_l = [2(l + \tfrac{1}{2})/s]^{\frac{1}{2}}. \qquad (5)$$

The density of states in the lth magnetic sub-band is given by

$$N_l(\epsilon) = 2(s/2\pi)(2m^*/h^2)^{\frac{1}{2}} |\epsilon - \epsilon_l|^{-\frac{1}{2}} = (s/2\pi)N^{(1)}(\epsilon), \qquad (6)$$

where ϵ_l is the energy at the edge of the lth sub-band. We note that the density of states at the edge of each one-dimensional sub-band is infinite, a consequence of the one-dimensional character of the sub-bands; this is in contrast to the zero density of states at the edge of the three-dimensional energy band in the absence of a magnetic field (Fig. 2). The ratio of the density of states in a magnetic sub-band to the density of states in the corresponding energy band in the absence of a magnetic field is given by

$$N_l(\epsilon)/N^{(3)}(\epsilon) = \hbar\omega_0/2|\epsilon|, \qquad (7)$$

where ϵ is measured relative to the band edges. The density of states of the sub-bands is thus higher than that for the normal band for values of $|\epsilon|$ less than $\frac{1}{2}\hbar\omega_0$.

In an actual semiconductor the energy bands in the absence of a magnetic field may be degenerate at one or more points in k space and so may not be simple in the sense defined above. A particularly important case is that in which two or more bands are degenerate at $\mathbf{k}=0$.
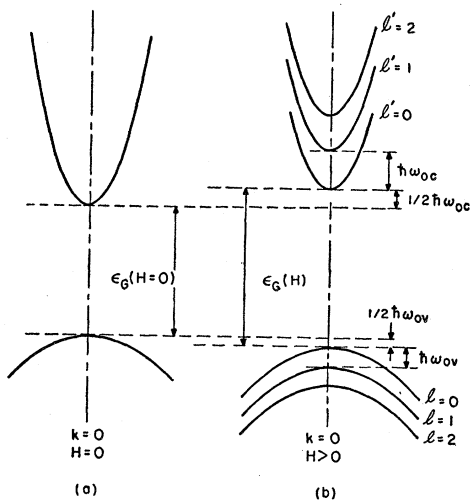
[8] M. H. Johnson and B. A. Lippman, Phys. Rev. **76**, 828 (1949).

One may characterize such bands by the angular momentum quantum numbers J and M which describe the atomic states obtained from the Bloch functions at $\mathbf{k}=0$ in the tight binding limit. The quantum number J specifies the total angular momentum and M specifies the component of angular momentum parallel to some particular axis. In the presence of an external magnetic field the degenerate bands give rise to a multiplicity of magnetic sub-bands which can be labeled by the magnetic quantum number l in addition to the quantum numbers J and M.

In energy bands arising from s-type atomic levels, the energy levels are doubly degenerate at all points in k-space corresponding to the two possible orientations of the electronic spin, and are characterized by a J value of $+\frac{1}{2}$ and by M values of $+\frac{1}{2}$ and $-\frac{1}{2}$. In the presence of a magnetic field, each of the doubly degenerate levels is split into two levels corresponding to the two values $+\frac{1}{2}$ and $-\frac{1}{2}$ of M. Thus, for an s-type conduction band, the energy levels of the corresponding one-dimensional
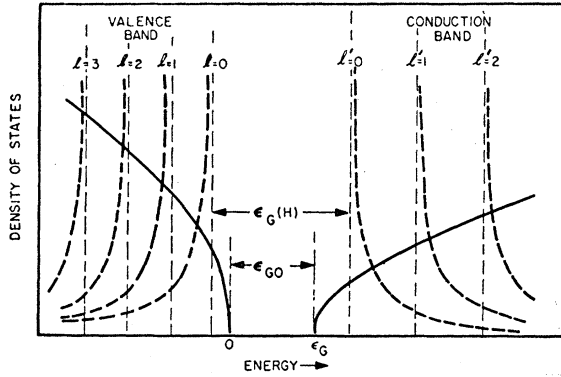

FIG. 2. Densities of states for a simple semiconductor for $H=0$ (solid lines) and for $H>0$ (heavy dashed lines).

sub-bands are given by[9]

$$\epsilon_c(k_z,l,M) = \epsilon_c + \hbar^2 k_z^2/2m_c^* + (l+\tfrac{1}{2})\hbar\omega_0 + g\beta H M, \quad (8)$$

where g is the effective g factor for the carriers, and $\beta = e\hbar/2mc$ is the Bohr magneton. The energy separation between the $M=+\frac{1}{2}$ and the $M=-\frac{1}{2}$ sub-bands having the same l magnetic quantum number is $g\beta H$. In the case of degenerate valence bands in which there are orbital as well as spin contributions to the total angular momentum, and in which there are also spin-orbit interaction effects, the character of the energy levels in the presence of an external magnetic field is much more complicated and is treated in Sec. 3.

Cyclotron resonance (CR) in a simple s-type energy band involves vertical ($\Delta k_z = 0$) optical transitions between magnetic sub-bands with the same M but having l values differing by one, and takes place to first order
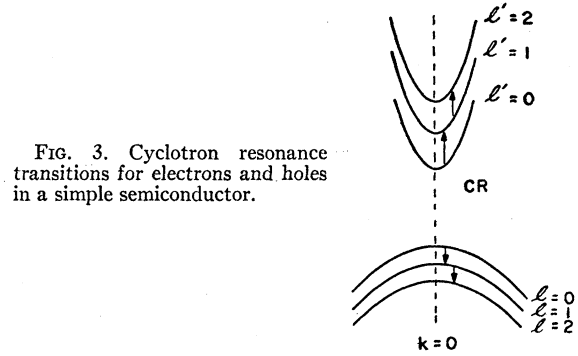

FIG. 3. Cyclotron resonance transitions for electrons and holes in a simple semiconductor.

only when the electric vector of the radiation field is perpendicular to the direction of the applied magnetic field, $E \perp H$, (Fig. 3). For simple energy bands the width of the cyclotron resonance absorption bands is determined only by the broadening of the individual energy levels. The condition for obtaining a well-defined CR absorption band is that the width of the energy levels be smaller than the vertical energy separation between adjacent sub-bands, namely that $\Delta\epsilon < \hbar\omega_0$, where $\Delta\epsilon = \hbar/\tau$ and τ is the lifetime of a carrier in a given level which is generally determined by scattering processes. This yields the condition $\omega_0\tau > 1$ which corresponds classically to the requirement that on the average the carriers complete at least $1/2\pi$ of their circular orbits about the magnetic field between collisions.

B. Optical Transitions between Simple Valence and Conduction Bands for Zero Magnetic Field

In the absence of a magnetic field the intrinsic absorption constant for vertical transitions between a "simple" valence band n and a "simple" conduction band n' has the form[10]

$$a_{nn'}(\omega) = \frac{\alpha\hbar^2|I_{nn'}|^2}{\eta m^2\hbar\omega}\bar{N}_{nn'};$$

$$\bar{N}_{nn'} = 4\pi\left(\frac{2\bar{m}^*}{\hbar^2}\right)^{\frac{3}{2}}(\hbar\omega - \epsilon_{nn'})^{\frac{1}{2}}, \quad (9)$$

where $\bar{N}_{nn'}$ is the reduced effective density of states, α is the fine structure constant; η is the refractive index at ω, $\bar{m}^* = m_n^* m_{n'}^*/(m_n^* + m_{n'}^*)$ is the reduced effective mass, $I_{nn'}$ is the momentum matrix element for vertical optical transitions, $\epsilon_{nn'}$ is the energy separation between the two band edges, and $\hbar\omega$ is the energy of the photons. For transitions allowed to first order in effective-mass theory, the matrix element does not vary appreciably with k and may be assumed constant. Under these conditions the absorption constant is zero at the absorption edge (i.e., at $\hbar\omega = \epsilon_{nn'}$), varies as $(\hbar\omega - \epsilon_{nn'})^{\frac{1}{2}}$ near the edge, and varies as $(\hbar\omega)^{-\frac{1}{2}}$ far beyond the edge (Fig. 4).

---

[9] Equation (8) may also be applied to the V_3 valence band of germanium which is split away from the top of the valence band by spin-orbit coupling.

[10] D. L. Dexter, *Photoconductivity Conference* (John Wiley and Sons, Inc., New York, 1956), p. 155.
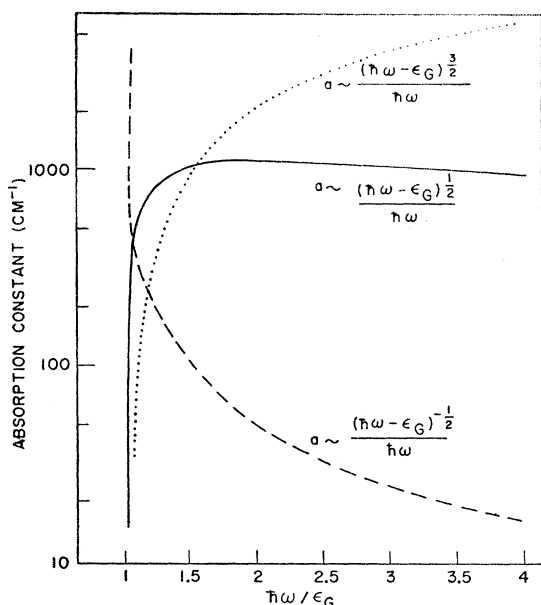
FIG. 4. Possible types of frequency dependence for the absorption constant.

It should be noted that the absorption constant at the absorption edges is zero because the density of states vanishes at the edges of three-dimensional energy bands.

The shape of the absorption spectrum will be modified by broadening of the energy levels. On the assumption that each electronic transition is broadened according to the Lorentz theory of line shape, the intrinsic absorption constant will have the form

$$a_{nn'}(\omega)=\frac{\alpha h^2}{\eta m^2}|I_{nn'}|^2 4\pi\left(\frac{2m^*}{h^2}\right)^{\frac{3}{2}}\frac{1}{(\hbar\omega)^2+(\Delta\epsilon)^2}$$

$$\times\left\{\left[(\hbar\omega-\epsilon_{nn'})^2+(\Delta\epsilon)^2\right]^{\frac{1}{4}}\left[\hbar\omega\begin{pmatrix}\cos(\varphi/2)\\\sin(\varphi/2)\end{pmatrix}\right.\right.$$

$$\left.\left.+\Delta\epsilon\begin{pmatrix}\sin(\varphi/2)\\\cos(\varphi/2)\end{pmatrix}\right]-\Delta\epsilon(\epsilon_{nn'})^{\frac{1}{2}}\right\}, \quad (10)$$

where $\varphi=$arc $\tan[\Delta\epsilon/(\hbar\omega-\epsilon_{nn'})]$; the upper choice of the trigonometric function applies when $\hbar\omega$ is larger than $\epsilon_{nn'}$ and the lower choice applies when $\hbar\omega$ is smaller than $\epsilon_{nn'}$. Thus, broadening causes the absorption edge to extend to photon energies below the energy gap, i.e., the absorption edge is smeared out. For values of $\hbar\omega-\epsilon_{nn'}$ large compared to $\Delta\epsilon$, the expression reduces to the one in which broadening is neglected. The effect of broadening is thus pronounced only at the absorption edge.

When the vertical optical transitions between the two bands are only allowed to second order, the matrix

element $I_{nn'}$ will have the form[11]

$$I_{nn'}{}^{(2)}(\beta)=\frac{k_\alpha}{m}\left[\sum_{n''\neq n'}\frac{p_{nn''}{}^\beta p_{n''n'}{}^\alpha}{\omega_{n''n'}}\right.$$

$$\left.+\sum_{n''\neq n}\frac{p_{nn''}{}^\alpha p_{n''n'}{}^\beta}{\omega_{n''n}}\right], \quad (11)$$

where $p_{nn''}$ is the matrix element of the momentum operator with respect to the Bloch functions at $\mathbf{k}=0$ for bands n and n'', $\hbar\omega_{nn'}=\epsilon_n-\epsilon_{n'}$, n'' represents a third energy band which serves as an intermediate state, and the repeated index α is to be summed over x, y, z. The quantity $|I_{nn'}{}^{(2)}|^2$ is proportional to k^2 for transitions between parabolic bands, and is therefore proportional to $\hbar\omega-\epsilon_{nn'}$. The absorption constant will then have the form $a_{nn'}(\omega)\propto(\hbar\omega-\epsilon_{nn'})^{\frac{3}{2}}/\hbar\omega$. It will therefore be zero at the absorption edge, and will increase as $(\hbar\omega-\epsilon_{nn'})^{\frac{3}{2}}$ near the absorption edge and as $(\hbar\omega)^{\frac{1}{2}}$ far from the absorption edge (Fig. 4).

When one of the energy bands has its band edge away from $k=0$, the intrinsic absorption edge will involve nonvertical optical transitions via intermediate states with the simultaneous emission or absorption of phonons.[12] The absorption constant for such processes will be of second order and will consist of a superposition of terms of the form

$$a_{nn'}(\omega,n'',p)\propto|I_{nn''}|^2|I_{n''n'p}|^2(\hbar\omega-\epsilon_{nn'p})^2/\hbar\omega, \quad (12)$$

where $I_{nn''}$ is the matrix element for vertical optical transition between band n and an intermediate band n''; $I_{n''n'p}$ is the electron-lattice interaction matrix element involving phonon transitions between the intermediate band n'' and band n'; $\epsilon_{nn'p}=\epsilon_{nn'}\pm\epsilon_p$; ϵ_p is the energy of the particular type of phonon involved; and the $+$ choice indicates the emission of phonons while the $-$ choice indicates the absorption of phonons. Each of the absorption constant terms thus involves an additional factor of the form $(\hbar\omega-\epsilon_{nn'p})^{\frac{3}{2}}$ due to the participation of phonons via an intermediate state. When the vertical transitions between the initial and the intermediate state are forbidden so that $|I_{nn''}|^2$ is itself proportional to k^2, the terms in the absorption constant will have the form

$$a_{nn'}(\omega)\propto(\hbar\omega-\epsilon_{nn'p})^3/\hbar\omega. \quad (13)$$

When vertical optical transitions occur between two valence bands or between two conduction bands, the absorption constant will obviously depend on the concentration of free carriers in the two bands under consideration, as well as on the character of the energy bands involved. In addition, depending on the relative magnitude of the effective masses of the two bands involved, $\epsilon_{nn'}$ may be either a minimum separation or a

[11] A. Kahn, Phys. Rev. 97, 1647 (1955); E. O. Kane, J. Phys. Chem. Solids 1, 83 (1956).
[12] Bardeen, Blatt, and Hall, Photoconductivity Conference (John Wiley and Sons, Inc., New York, 1956), p. 146.

maximum separation. Thus in the case of the V_1 to V_3 transitions in germanium where $m_1^* > m_3^*$, the ϵ_{13} corresponds to a minimum separation of the two bands and the absorption spectrum exhibits a long-wavelength limit. On the other hand in the case of the V_2 to V_3 transitions where $m_2^* < m_3^*$, the ϵ_{23} corresponds to a maximum separation of the two bands and the absorption spectrum exhibits a short-wavelength limit.

C. Optical Transitions between Simple Valence and Conduction Bands in Externally Applied Magnetic Fields

In the presence of a magnetic field, two interband magneto-optical effects may be expected to occur: (1) the optical gap will change, and (2) the intrinsic absorption spectrum will change in character and under appropriate conditions may be expected to exhibit structure due to transitions between magnetic sub-bands in the valence band and those in the conduction band (Fig. 5).

According to Eq. (8) the minimum separation between a simple valence and a simple conduction band in the presence of a magnetic field is given by[13]

$$\epsilon_{nn'}(H) = \epsilon_{nn'} + \tfrac{1}{2}(\hbar\omega_{0n} + \hbar\omega_{0n'}) - \tfrac{1}{2}(|g_n| + |g_{n'}|)\beta H. \quad (14)$$

Depending on the relative magnitudes of the effective masses and the g factors involved, the magnetic field may cause either an increase or a decrease in the energy gap between the two bands which will manifest itself as a shift of the optical absorption edge either to shorter or to longer wavelengths, respectively. In general the term involving the cyclotron frequencies will be larger than the term involving the g factors and the effect of magnetic field will be to increase the band gap.

Vertical electronic transitions from sub-band l, M in the valence band to sub-band l', M' in the conduction band give rise to an optical absorption band characterized by an absorption constant depending on photon frequency according to the relation:

$$a_{ll'}(\omega) = \frac{2\alpha\hbar^2}{\eta m^2}\left(\frac{eH}{hc}\right)\left(\frac{2\bar{m}^*}{h^2}\right)^{\frac{1}{2}}|I_{ll'}|^2 \frac{(\hbar\omega - \epsilon_{ll'})^{-\frac{1}{2}}}{\hbar\omega}$$

$$= \frac{\alpha\hbar^2}{\eta m^2}\frac{\bar{N}_{ll'}|I_{ll'}|^2}{\hbar\omega}, \quad (15)$$

where we have omitted the subscripts designating the M quantum numbers of the sub-bands involved. Level broadening is not included in this expression. $\bar{N}_{ll'}$ is the reduced effective density of states for the two sub-bands, $\epsilon_{ll'}$ is the corresponding energy gap, given by

$$\epsilon_{ll'} = \epsilon_{nn'} + (l+\tfrac{1}{2})\hbar\omega_{0n} + (l'+\tfrac{1}{2})\hbar\omega_{0n'}$$
$$- g_n\beta HM + g_{n'}\beta HM'. \quad (16)$$

---

[13] Equation (14) is applicable for example to the separation between the V_3 valence band and the Γ_2 conduction band in germanium.
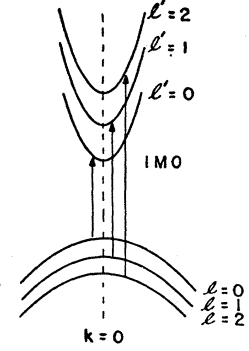

FIG. 5. Interband transitions for a simple semiconductor in the presence of a magnetic field.

The magnitudes of the momentum matrix elements $I_{ll'}$ will, in general, be governed by appropriate selection rules involving the state of polarization of the radiation, the direction of propagation of the radiation, and the direction of the applied magnetic field, as well as by the character of the valence and conduction bands.

For allowed first-order transitions in which $I_{ll'}$ is effectively independent of k, $a_{ll'}(\omega)$ will be infinite at the absorption edge (i.e., at $\hbar\omega = \epsilon_{ll'}$), and decrease as $(\hbar\omega - \epsilon_{ll'})^{-\frac{1}{2}}$ near the edge, and as $(\hbar\omega)^{-\frac{3}{2}}$ far from the edge (Fig. 4). The infinity in the absorption constant at the absorption edge is typical of allowed interband transitions between one-dimensional energy bands, and arises from the infinities in the densities of states at the band edges of one-dimensional bands, just as the zero absorption constant at the absorption edge for interband transitions between energy bands in the absence of a magnetic field arises from the zeros in the densities of states at the band edges of three-dimensional energy bands.

In real crystals, energy level broadening will remove the infinities at the absorption edges. If we assume that each transition is broadened according to a Lorentz shape, the absorption constant for vertical interband transitions between magnetic sub-bands of the valence and conduction bands will have the form

$$a_{ll'}(\omega) = \frac{2\alpha\hbar^2}{\eta m^2}\left(\frac{eH}{hc}\right)\left(\frac{2\bar{m}^*}{h^2}\right)^{\frac{1}{2}}|I_{ll'}|^2\frac{1}{(\hbar\omega)^2 + (\Delta\epsilon)^2}$$

$$\times\left\{[(\hbar\omega - \epsilon_{ll'})^2 + (\Delta\epsilon)^2]^{-\frac{1}{4}}\left[\hbar\omega\begin{pmatrix}\cos(\varphi/2)\\\sin(\varphi/2)\end{pmatrix}\right.\right.$$

$$\left.\left. - \Delta\epsilon\begin{pmatrix}\sin(\varphi/2)\\\cos(\varphi/2)\end{pmatrix}\right] + \Delta\epsilon(\epsilon_{nn'})^{-\frac{1}{2}}\right\}, \quad (17)$$

where again the upper choice of the trigonometric function applies when $\hbar\omega$ is larger than $\epsilon_{ll'}$ and the lower choice applies when $\hbar\omega$ is smaller than $\epsilon_{ll'}$. As a result of energy level broadening, the absorption constant for a given pair of sub-bands will peak at a photon energy $\simeq 0.58\Delta\epsilon$ higher than that corresponding to the energy gap. The magnitude of the absorption constant at the
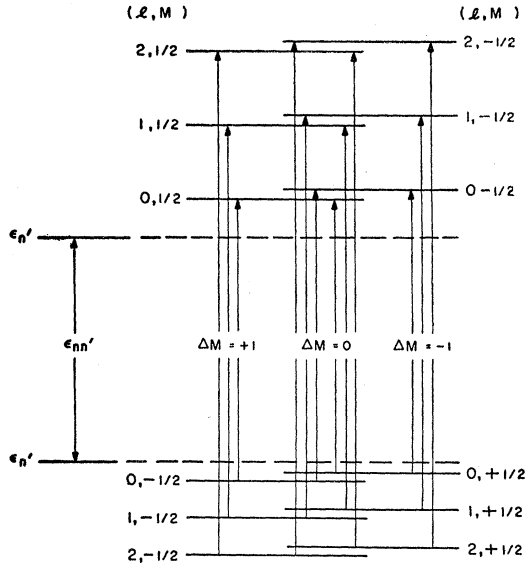
FIG. 6. Interband transitions and ΔM selection rules for a simple semiconductor in the presence of a magnetic field. The g factor of the electrons in the conduction band is taken as negative, and only the energies at $k_z = 0$ are indicated.

peak will be proportional to H. It will also be proportional to $(\Delta \epsilon)^{-\frac{1}{2}}$ and therefore to $\tau^{\frac{1}{2}}$. For values of $(\hbar \omega - \epsilon_{ll'})$ large compared to $\Delta \epsilon$, the above expression for $a_{ll'}(\omega)$ reduces to the one given in Eq. (15) in which broadening is neglected, i.e., the effect of broadening of the levels is only pronounced at the absorption edge.

It is of interest to note that the difference in the shapes of the CR and IMO spectra arises from the optical transitions between states for which $k_z \neq 0$. If one considers only the transitions for $k_z = 0$, CR and IMO transitions both yield line spectra. When $k_z \neq 0$ transitions are included, the IMO absorption lines become extended absorption bands of the type discussed above whereas the CR lines are not affected. The tails to the extended IMO absorption bands result from the quasi-continuous nature of the energy bands in the z direction, and the different curvatures (in sign as well as in magnitude) of the valence and conduction bands. The CR absorption spectrum, on the other hand, remains unchanged in character, since, in the simple model considered here, adjacent sub-bands have the same curvature. In the cases where the energy bands deviate from a simple parabolic dependence on k, the separation of adjacent sub-bands will vary with k_z and will manifest itself in an asymmetrical broadening of the CR absorption band and in a modification of the tails to the IMO absorption peaks. The above discussion remains essentially unchanged if Lorentz broadening is included. The CR lines will be symmetrically broadened but will have the same shape whether or not $k_z \neq 0$ transitions are included. For nonparabolic energy bands there will be additional asymmetrical broadening. The effect of Lorentz broadening on the IMO lines will be primarily

to alter their shape in the vicinity of their edges, as discussed previously.

The selection rules for the first-order IMO effect are $\Delta l = 0$ and $\Delta M = 0, \pm 1$ (see Sec. 2D). This is illustrated in Fig. 6 for a semiconductor with simple valence and conduction bands both of which are characterized by $M = +\frac{1}{2}$ and $-\frac{1}{2}$. The corresponding IMO spectrum for simple energy bands therefore consists of the superposition of the individual absorption bands for the various initial values of the magnetic quantum numbers l and M. The positions of the absorption peaks can be obtained from Eq. (16). A typical first-order $\Delta l = 0$, $\Delta M = +1$ IMO spectrum for a semiconductor with simple energy bands is shown in Fig. 7 together with the corresponding intrinsic absorption spectrum in the absence of a magnetic field. The separation between adjacent peaks is given by $\hbar \omega_{0n} + \hbar \omega_{0n'}$. The IMO spectrum rises above and falls below the zero-field intrinsic absorption spectrum. The $\Delta M = -1$ spectrum also consists of a set of uniformly spaced absorption peaks, with the first peak displaced from that for the $\Delta M = +1$ spectra by $|g_n + g_{n'}|\beta H$.

The corresponding $\Delta M = 0$ spectrum will consist of the superposition of two sets of uniformly spaced absorption peaks displaced with respect to one another by $|g_n - g_{n'}|\beta H$. The separation between adjacent peaks in each set is again simply $\hbar \omega_{0n} + \hbar \omega_{0n'}$. The various IMO spectra for the simple semiconductors are shown schematically in Fig. 8. IMO spectra will obviously be considerably more complicated when degenerate energy bands are involved. These will be discussed in Sec. 3.

The second-order matrix elements for IMO spectra $I_{nn'}^{(2)}$ will in general include terms involving $\Delta l = 0$ which are proportional to k_z as well as terms involving $\Delta l = \pm 1$ which are independent of k_z (see Sec. 2D). The selection rules require further that $\Delta M = 0, \pm 1, \pm 2$ and that $\Delta l + \Delta M = 0, \pm 1$. The $\Delta l = \pm 1$ terms yield peaked
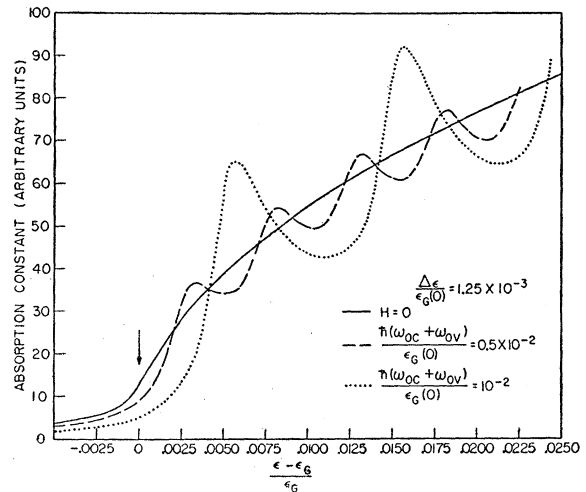

FIG. 7. Interband absorption spectrum for a simple semiconductor for $H = 0$ and for $H > 0$.

absorption spectra of the form given by Eq. (17). The magnitude of the absorption peaks will be determined by matrix elements for vertical transitions involving states in intermediate bands and will be proportional to $H^2\tau^{\frac{1}{2}}l'$, where l' is the larger of the two l quantum numbers involved. The $\Delta l = 0$ terms, on the other hand, which are proportional to k_z, will yield absorption spectra in which the absorption constant varies as $(\hbar\omega - \epsilon_{ll'})^{\frac{1}{2}}/\hbar\omega$ and will therefore exhibit no absorption peaks. The second-order IMO absorption spectra will, of course, consist of a superposition of the two types of spectra and will be much more complicated than the first-order IMO spectra.

When the extremum of one of the energy bands is not at the center of the Brillouin zone (i.e., it is at some point $k \neq 0$), the intrinsic absorption edge will involve nonvertical optical transitions and the simultaneous emission or absorption of phonons. In the presence of a magnetic field, the absorption or emission of phonons introduces an additional factor of the form $(\hbar\omega - \epsilon_{ll'p})^{\frac{1}{2}}$ into the expression for the absorption constant. The absorption constant for the indirect transitions between a pair of magnetic sub-bands will accordingly be of the form

$$a_{ll'}(\omega, l'', p) \propto |I_{ll''}|^2 |I_{l''l'p}|^2 (\hbar\omega - \epsilon_{ll'p})^0/\hbar\omega, \quad (18)$$

where $I_{ll''}$ is the matrix element for direct optical transitions between sub-band l and an intermediate sub-band l'', $I_{l''l'p}$ is the electron-lattice interaction matrix element involving phonon transitions between the intermediate sub-band l'' and sub-band l', and $\epsilon_{ll'p} = \epsilon_{ll'} \pm \epsilon_p$. When the matrix element $I_{ll''}$ for the optical transitions via the intermediate sub-bands l'' is constant, the corresponding absorption constant terms will have finite values at their respective absorption edges, i.e., at $\hbar\omega = \epsilon_{ll'p}$. On the other hand, when a given term in the matrix element is proportional to k, the corresponding term in the absorption constant will be of the form

$$a_{ll'}(\omega) \propto (\hbar\omega - \epsilon_{ll'p})/\hbar\omega. \quad (19)$$

The absorption constant will be zero at the absorption edge, increase as $(\hbar\omega - \epsilon_{ll'p})$ near the edge, and be independent of $\hbar\omega$ far from the edge.

The IMO spectrum for indirect transitions will thus be a complicated superposition of spectra for each type of intermediate state and type of phonon transition involved. For matrix elements which are allowed to first order, the structure in the indirect transition IMO spectrum may be expected to be less pronounced than in the case of direct transition IMO spectra, but should nevertheless be observable. It may also be possible to observe additional broad peaks in the IMO spectrum due to direct transitions between the energy bands. These would arise because, at the point k where one of the bands has an extremum, the densities of states in the magnetic sub-bands would be infinite, whereas in the sub-bands of the other band (whose extremum is at
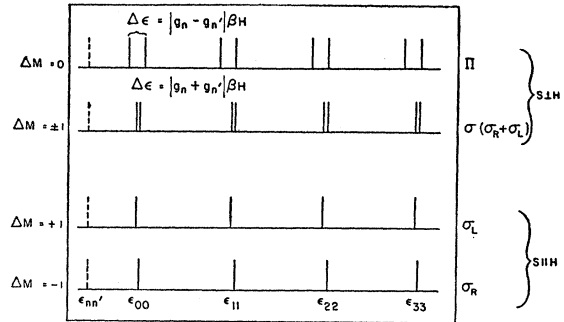

FIG. 8. Position of the IMO absorption peaks for various types of polarized light corresponding to the transitions shown in Fig. 6.

$k = 0$), the density of states would have some finite value at k.

D. Matrix Elements for Interband Transitions in the Presence of Magnetic Field

In the previous section we have discussed the character of IMO spectra emphasizing effects arising from effective densities of states and introducing the pertinent matrix elements essentially as phenomenological factors. We now wish to discuss the IMO matrix elements and the associated selection rules and polarization effects.

Let us first consider the case of two simple energy bands, n and n' which are nondegenerate, except for spin, spherically symmetric and parabolic with extreme at $k = 0$. We shall neglect spin-orbit coupling effects. The wave functions of the carriers which are obtained from the effective mass formalism of Luttinger and Kohn[14] can be written to second order as

$$\psi_n(\mathbf{r}) = F_n(\mathbf{r})\varphi_n(\mathbf{r}) - \left(\frac{1}{m\hbar}\right)$$
$$\times \left[\sum_{n'' \neq n} (p_{n''n}{}^\alpha/\omega_{n''n})P_\alpha F_n(\mathbf{r})\right]\varphi_{n''}(\mathbf{r}), \quad (20)$$

with a similar equation for band n' obtained by replacing n by n'. The functions $\varphi_n(\mathbf{r})$ are the Bloch functions for band n at $k = 0$; P_α is the α component of the kinetic momentum operator $\mathbf{P} = \mathbf{p} + (e/c)\mathbf{A}$, where $\mathbf{A}$ is the vector potential for the external magnetic field. The repeated index α in Eq. (20) is summed over x, y, z. The functions $F_n(\mathbf{r})$ are the wave functions for a free electron in a constant magnetic field. If the gauge $\mathbf{A} = (-yH, 0, 0)$ is chosen, the functions $F_n(\mathbf{r})$ are given aside from normalization factors by

$$F_n(\mathbf{r}) = G_l(t) \exp[i(k_x x + k_z z)], \quad (21)$$

where $G_l(t)$ is the harmonic oscillator function of the variable $t = s^{\frac{1}{2}}[y - k_x/s]$. For band n' the functions $F_{n'}(\mathbf{r})$ will have the form given by Eq. (21) except that k_x, k_z, l are replaced by k_x', k_z', l'.

The matrix elements which characterize the optical

---
[14] J. M. Luttinger and W. Kohn, Phys. Rev. **97**, 869 (1955).

transitions between bands n and n' in the presence of a static externally applied magnetic field H_z are of the form

$$I_\beta = \int \psi_n^*(\mathbf{r}) P_\beta \psi_{n'}(\mathbf{r}) d\mathbf{r}, \tag{22}$$

where we have dropped subscripts n and n' on I_β for simplicity.

If we consider only first-order terms in the wave function, the matrix elements would have the form

$$I_\beta^{(1)} = \int F_n^*(\mathbf{r}) \left(p_\beta + \frac{e}{c} A_\beta \right) F_{n'}(\mathbf{r}) d\mathbf{r} \int \varphi_n^*(\mathbf{r}) \varphi_{n'}(\mathbf{r}) d\mathbf{r}$$

$$+ \int F_n^*(\mathbf{r}) F_{n'}(\mathbf{r}) d\mathbf{r} \int \varphi_n^*(\mathbf{r}) p_\beta \varphi_{n'}(\mathbf{r}) d\mathbf{r}. \tag{23}$$

Because of the orthogonality of the Bloch functions of different energy bands, the first term is nonzero only for transitions between states in the same energy bands. The second term is nonzero for direct transitions between states in different energy bands for which there exists a nonzero matrix element of the operator p in the absence of a magnetic field, i.e., for which

$$\mathbf{p}_{nn'} = \frac{(2\pi)^3}{\Omega} \int_{\text{cell}} \varphi_n^*(\mathbf{r}) \mathbf{p} \varphi_{n'}(\mathbf{r}) d\mathbf{r}$$

is nonzero (Ω is the volume of a unit cell).[15] The first term is thus responsible for CR transitions in a magnetic field while the second term is responsible for the IMO transitions.

From the character of the wave functions $F_n(r)$ for different quantum numbers, it follows from the first integral of the CR term that the first-order selection rules for CR transitions are $\Delta k_x = 0$, $\Delta k_z = 0$ (the condition for vertical transitions) and $\Delta l = \pm 1$.

The magnitudes of the CR $(E \perp H)$ matrix elements $I_x^{(1)}$ and $I_y^{(1)}$ are given as follows[16]:

$$I_x^{(1)} = -\hbar s^{\frac{1}{2}} [(l+1)/2]^{\frac{1}{2}},$$
$$I_y^{(1)} = +i\hbar s^{\frac{1}{2}} [(l+1)/2]^{\frac{1}{2}}. \tag{24}$$

For $E \| H$, the selection rules are that k_x, k_z, and l remain unchanged and $I_z^{(1)} = \hbar k_z$. However, since one must remain in the same band, this corresponds to transition between states of the same energy and does not lead to any absorption.

From the first integral of the IMO term it follows that the selection rules for the first-order IMO transitions are $\Delta k_x = 0$, $\Delta k_z = 0$ (vertical transitions), and $\Delta l = 0$. Additional selection rules are specified by the nature of the Bloch functions $\varphi_n(r)$ and $\varphi_{n'}(r)$. These functions have

symmetry properties which are related to the angular momentum character of the atomic states to which they would reduce in the tight-binding limit; they are characterized by values of J, the total angular momentum, and M, the component of the total angular momentum in the direction of the external magnetic field. The selection rules for M are that $\Delta M = 0$, or ± 1.

Associated with the selection rule $\Delta M = 0$, ± 1 are characteristic polarization effects. For light propagating along the external magnetic field (Poynting vector parallel to the external magnetic field and therefore $E \perp H$), the $\Delta M = +1$ transitions occur for left circularly polarized radiation (they correspond to the σ_L transition in atomic Zeeman spectra), and the $\Delta M = -1$ transitions occur for right circularly polarized radiation (they correspond to the σ_R transition in atomic Zeeman spectra). The $\Delta M = 0$ transitions do not occur for this configuration of the Poynting vector and the external magnetic field.

For light propagating perpendicular to the external magnetic field (Poynting vector perpendicular to this magnetic field) the $\Delta M = 0$ transitions occur for plane-polarized radiation with $E \| H$ (these correspond to the π transitions in atomic Zeeman spectra). Both the $\Delta M = +1$ and $\Delta M = -1$ transitions occur for plane-polarized radiation with $E \perp H$ (Fig. 9).

When we include second-order terms in the wave function, the optical matrix elements for IMO transitions are given by[17,18]

$$I_\beta = I_\beta^{(1)} + I_\beta^{(2a)} + I_\beta^{(2b)},$$

$$I_\beta^{(1)} = p_{nn'}^\beta \int F_n^*(\mathbf{r}) F_{n'}(\mathbf{r}) d\mathbf{r},$$

$$I_\beta^{(2a)} = -\frac{1}{\hbar m} \left[\sum_{n'' \neq n'} \frac{p_{nn''}^\beta p_{n''n'}^\alpha}{\omega_{n''n'}} + \sum_{n'' \neq n} \frac{p_{nn''}^\alpha p_{n''n}^\beta}{\omega_{n''n}} \right] \tag{25}$$

$$\times \int F_n^*(\mathbf{r}) \left[p_\alpha + \frac{e}{c} A_\alpha \right] F_{n'}(\mathbf{r}) d\mathbf{r},$$

$$I_\beta^{(2b)} = \frac{e}{imc} \frac{p_{nn'}^\alpha}{\omega_{nn'}} \int F_n^*(\mathbf{r}) \left[\frac{\partial A_\alpha}{\partial x_\beta} - \frac{\partial A_\beta}{\partial x_\alpha} \right] F_{n'}(\mathbf{r}) d\mathbf{r}.$$

We now discuss the relative magnitudes of the quantities I_β. As pointed out earlier, the term $I_\beta^{(1)}$ gives a contribution only if the zero-field direct transition between bands n and n' is allowed. Since $I_\beta^{(2b)}$ also is proportional to $p_{nn'}$, it will similarly make a contribution only if the zero-field direct transition is allowed. The integral in $I_\beta^{(2b)}$ yields zero for $\beta = z$, $+H$ for $\beta = x$ and $-H$ for $\beta = y$. Consequently, $I_\beta^{(2b)}$ differs in magnitude from $I_\beta^{(1)}$ by a factor of 0 or $(eH/mc)/\omega_{nn'}$. Noting

---

[15] The term eA/c does not appear with p in the second-term integral containing the Bloch functions since A is not a differential operator and is nonperiodic. The A is lumped together with the modulating function.

[16] R. B. Dingle, Proc. Roy. Soc. (London) A212, 38 (1952).
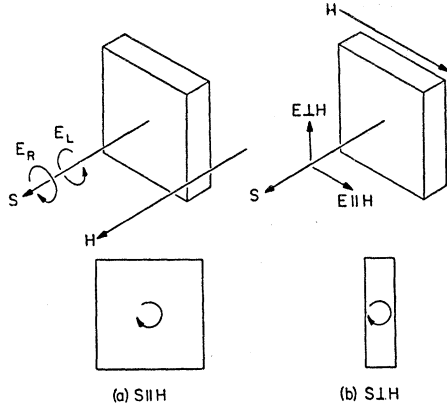
[17] Blatt, Wallis, and Burstein, Bull. Am. Phys. Soc. Ser. II, 2, 141 (1957).

[18] Second-order matrix elements for cyclotron resonance transitions are treated by R. F. Wallis [J. Chem. Phys. Solids 4, 101 (1958)].

FIG. 9. Relative orientations of sample, electric vector E, Poynting vector S, and magnetic field H.

FIG. 10. Energy band diagrams for Ge (a) and for InSb (b).

that m is the mass of an electron in free space, we see that for presently available fields $I_\beta^{(2b)}$ will be negligible compared to $I_\beta^{(1)}$ for the semiconductors which have been studied to date. Indeed, if $(eH/mc)/\omega_{nn'}$ were not negligible compared to unity, the perturbation procedure would be suspect.

The term $I_\beta^{(2a)}$ corresponds to the second-order matrix element for zero magnetic field given by Eq. (11), with the integral involving the modulating functions $F_n(r)$ replacing the factor k. The contribution of $I_\beta^{(2a)}$ depends on whether or not the crystal has a center of symmetry. If a center of symmetry exists, as in Ge, then the bands n and n' must have different parity in order for the first-order term $I_\beta^{(1)}$ to contribute. For example, the vertical transitions between the valence bands V_1, V_2, or V_3 and the conduction band Γ_2 in Ge [Fig. 10(a)] are allowed. For this case, however, the second-order term $I_\beta^{(2a)}$ vanishes because any intermediate band n'' must have the same parity as either n or n' and the corresponding momentum matrix element must be zero. On the other hand, if the bands n and n' have the same parity so that $I_\beta^{(1)}$ vanishes, as in the case of transitions between the V_1 band and the V_3 band in Ge, then intermediate states n'', such as the Γ_2 band, having parity opposite to n and n' may exist so that the second-order term $I_\beta^{(2a)}$ does not vanish.

If a center of symmetry does not exist, then the bands n and n' no longer can be classified according to parity and nonzero contributions may arise from both $I_\beta^{(1)}$ and $I_\beta^{(2a)}$. For InSb, which lacks a center of symmetry, transitions are allowed between the V_1, V_2, and V_3 valence band having Bloch functions at $k=0$ belonging to the representation Γ_4, and the conduction band having a Bloch function at $k=0$ belonging to the representation Γ_1 [Fig. 10(b)]. Furthermore, the selection rules given by Dresselhaus[19] indicate that the second-order term $I_\beta^{(2a)}$ may be nonzero when the intermediate state has Bloch functions at $k=0$ belonging to the representation Γ_4. It may be pointed out that in

[19] G. Dresselhaus, Phys. Rev. 100, 580 (1955).

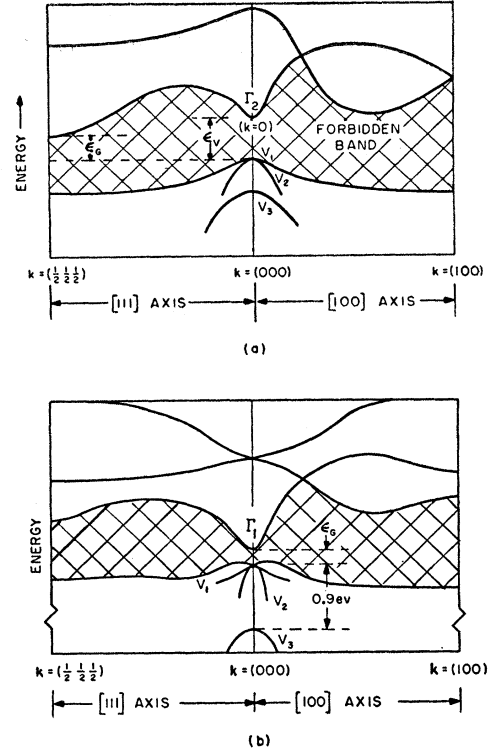the theory of cyclotron resonance absorption[6] a term analogous to $I_\beta^{(2a)}$ gives by far the largest contribution to the absorption in InSb. For the IMO effect, it is not yet clear just how large the contribution from $I_\beta^{(2a)}$ is. We wish to mention that Eqs. (20), (23), and (25) neglect effects arising from the degeneracy of the valence bands which will be discussed in the next section.

The selection rules and polarization effects arising from $I_\beta^{(2a)}$ are much more complex than those from $I_\beta^{(1)}$. The integral involving the moldulating functions has the same form as that appearing in the first-order term for CR transitions and yields the selection rules $\Delta l = \pm 1$, 0 and $\Delta k_x = 0$, $\Delta k_z = 0$. The contributions to $I_\beta^{(2a)}$ for $\Delta l = 0$ are proportional to k_z and are independent of l and H, whereas those for $\Delta l = \pm 1$ are independent of k_z and are proportional to $l^{\frac{1}{2}}$ or $(l+1)^{\frac{1}{2}}$ and to $H^{\frac{1}{2}}$.

The factor in $I_\beta^{(2a)}$ which involves the products of momentum matrix elements $p_{nn''}{}^\alpha p_{n''n'}{}^\beta$ and $p_{nn''}{}^\beta p_{n''n'}{}^\alpha$, yields the selection rule $\Delta M = 0$, ± 1, ± 2. The possibility of $\Delta M = \pm 2$ arises because the intermediate state n'' can have an M value differing by ± 1 from both the initial and final states n and n'. The values for Δl and ΔM are further restricted by a selection rule on their sum given by $(\Delta l + \Delta M) = 0$ or ± 1. This latter selection rule is consistent with the conservation of total angular momentum of electron and photon.

The $\Delta l = 0$ terms in $I_\beta^{(2a)}$ which are proportional to k_z lead to terms in the absorption coefficient which vary as

$(\hbar\omega-\epsilon_{ll'})^{\frac{1}{2}}$ and therefore do not yield absorption peaks. The $\Delta l=\pm1$ terms which are independent of k_z yield terms in the absorption constant which vary as $(\hbar\omega-\epsilon_{ll'})^{-\frac{1}{2}}$ and therefore lead to absorption peaks. However, unlike the first-order contributions to the absorption constant which are independent of l and proportional to the first power of H, these $\Delta l=\pm1$ contributions are proportional to l or $l+1$ and to the second power of H.

3. DEGENERATE ENERGY BANDS AND SPIN-ORBIT COUPLING

A. The V_1, V_2, and V_3 Valence Bands of Ge

Let us now consider the effects to be expected when one takes explicit account of spin-orbit coupling and the orbital degeneracy which exists in valence bands. In the absence of spin-orbit coupling and an external magnetic field, the valence band of the diamond structure semiconductors is sixfold degenerate at $\mathbf{k}=0$. The Bloch functions at $\mathbf{k}=0$ for the valence band pass into p-like atomic functions in the tight binding limit and consequently are threefold degenerate, while the remaining double degeneracy is a time-reversal degeneracy. Inclusion of spin-orbit coupling splits off a twofold degenerate band (the V_3 band). The remaining bands are fourfold degenerate at $\mathbf{k}=0$, but split into two twofold degenerate bands (the V_1 and V_2 bands) for $\mathbf{k}\neq0$. The separation Δ of the V_3 band from the V_1 and V_2 bands at $\mathbf{k}=0$ increases in the order C, Si, Ge, and Sn and is about 0.3 ev for Ge.

Following Luttinger,[20] we shall denote the valence band Bloch functions at $k=0$ by $\varphi_{\frac{3}{2}}^{(\frac{3}{2})}$, $\varphi_{\frac{1}{2}}^{(\frac{3}{2})}$, $\varphi_{-\frac{1}{2}}^{(\frac{3}{2})}$, and $\varphi_{-\frac{3}{2}}^{(\frac{3}{2})}$ for the V_1 and V_2 bands, and by $\varphi_{-\frac{1}{2}}^{(\frac{1}{2})}$ and $\varphi_{\frac{1}{2}}^{(\frac{1}{2})}$ for the V_3 band. The superscript specifies the value of the quantum number J for the corresponding atomic function in the tight binding limit, while the subscript specifies the value of the quantum number M. In terms of functions, X, Y, and Z which transform as x, y, z but are otherwise unspecified, the Bloch functions $\varphi_M^{(J)}$ can be written as

$$\varphi_{\frac{3}{2}}^{(\frac{3}{2})}=(1/\sqrt{2})(X+iY)\alpha,$$
$$\varphi_{\frac{1}{2}}^{(\frac{3}{2})}=(i/\sqrt{6})[(X+iY)\beta-2Z\alpha],$$
$$\varphi_{-\frac{1}{2}}^{(\frac{3}{2})}=(1/\sqrt{6})[(X-iY)\alpha+2Z\beta],$$
$$\varphi_{-\frac{3}{2}}^{(\frac{3}{2})}=(i/\sqrt{2})(X-iY)\beta,$$
$$\varphi_{\frac{1}{2}}^{(\frac{1}{2})}=(1/\sqrt{3})[(X+iY)\beta+Z\alpha],$$
$$\varphi_{-\frac{1}{2}}^{(\frac{1}{2})}=(i/\sqrt{3})[-(X-iY)\alpha+Z\beta],$$

(26)

where α and β are spin functions for spin up and spin down, respectively.

Luttinger and Kohn[14] and Luttinger[20] have developed an effective mass formalism for calculating the energy levels and wave functions of an electron or hole in a degenerate band with spin-orbit coupling and an external

magnetic field for a crystal with a center of symmetry. According to their theory the wave function for a given "magnetic" state, in the valence band of such a crystal, is given to first approximation by a linear combination of products of modulating functions $F(r)$ and Bloch function $\varphi_M^{(J)}$. The six modulating functions and the energy eigenvalues for a given state are obtained by solution of a set of six coupled differential equations. For magnetic fields ordinarily available in the laboratory, however, the mixing of $\varphi_M^{(\frac{3}{2})}$ and $\varphi_M^{(\frac{1}{2})}$ Bloch functions in Ge should be quite small, since the spacing of the magnetic levels is small compared to Δ. The modulating functions and the energies of the valence band magnetic states can then be determined by solving a set of four coupled differential equations for the V_1 and V_2 bands and a set of two differential equations for the V_3 band.

The set of coupled differential equations for the V_1 and V_2 bands involve a set of parameters γ_1, γ_2, γ_3, K and q defined by Luttinger,[20] as well as the propagation constant k_H parallel to the external magnetic field. The quantities γ_1, γ_2, and γ_3 are related to the effective mass parameters A, B, and C defined by Dresselhaus, Kip, and Kittel.[21] K is a so-called antisymmetric constant which arises from the noncommutability of the operators P_α and P_β (the kinetic momentum operators), and q is a constant arising from spin-orbit coupling. The solution of the four coupled equations is facilitated by taking the propagation constant $k_H=0$. This is particularly appropriate since the states which determine the peaks in the absorption spectrum in the presence of a magnetic field are those having $k_H=0$. An exact solution can now be given if $q=0$, and if $\gamma_2=\gamma_3$, the latter condition corresponding to $C=0$, or to the absence of warping of the V_1 and V_2 bands. Under these conditions, which are reasonably well satisfied for Ge, the wave functions for the magnetic states of the V_1 and V_2 bands in Ge can be written as linear combinations of two terms:

$$\psi_1^+=a_1G_{l-2}\varphi_{\frac{3}{2}}^{(\frac{3}{2})}+a_2G_l\varphi_{-\frac{1}{2}}^{(\frac{3}{2})}, \quad l\geq0$$
$$\psi_1^-=a_1'G_{l-2}\varphi_{\frac{1}{2}}^{(\frac{3}{2})}+a_2'G_l\varphi_{-\frac{3}{2}}^{(\frac{3}{2})}, \quad l\geq2$$
$$\psi_2^+=b_1G_{l-2}\varphi_{\frac{3}{2}}^{(\frac{3}{2})}+b_2G_l\varphi_{-\frac{1}{2}}^{(\frac{3}{2})}, \quad l\geq0$$
$$\psi_2^-=b_1'G_{l-2}\varphi_{\frac{1}{2}}^{(\frac{3}{2})}+b_2'G_l\varphi_{-\frac{3}{2}}^{(\frac{3}{2})}, \quad l\geq2$$

(27)

where a_1, a_2, $\cdots b_2'$ are numerical coefficients with a_1 and b_1 equal to zero for $l=0$ and $l=1$; G_l and G_{l-2} are the harmonic oscillator functions with quantum number l, and $l-2$, respectively. The corresponding energy eigenvalues consist of four sets of magnetic levels designated by $\epsilon_1^+(n)$, $\epsilon_2^+(n)$, $\epsilon_1^-(n)$ and $\epsilon_2^-(n)$, where $n=0, 1, 2, \cdots$ and are called ladders by Luttinger. The value of n is the larger of the two l values characterizing a given state. In the limit of large n, the levels in the $\epsilon_1^+(n)$ and $\epsilon_2^+(n)$ ladders approach a uniform spacing characteristic of the effective mass $m_2^*=0.04m$ for light holes, while the levels in the $\epsilon_1^-(n)$ and $\epsilon_2^-(n)$

[20] J. M. Luttinger, Phys. Rev. **102**, 1030 (1956).

[21] Dresselhaus, Kip, and Kittel, Phys. Rev. **98**, 368 (1955).

approach a uniform spacing characteristic of the effective mass $m_3{}^* = 0.3m$ for heavy holes. For small values of n, however, the four ladders show large deviations from uniform spacing (Fig. 11). It should be noted that each magnetic state is characterized by two (l,M) pairs of values: (n,M) and $(n-2, M+2)$, except for the two uppermost levels of each of the $\epsilon_1{}^+(n)$ and $\epsilon_2{}^+(n)$ ladders; the $\epsilon_1{}^+(0)$, $\epsilon_1{}^+(1)$, $\epsilon_2{}^+(0)$, and $\epsilon_2{}^+(1)$ magnetic states are characterized by only a single l and a single M: $(0, -\frac{1}{2})$ and $(1, -\frac{1}{2})$ for the $\epsilon_1{}^+$ ladder and $(0, -\frac{3}{2})$ and $(1, -\frac{3}{2})$ for the $\epsilon_2{}^+$ ladder.

The energy levels computed assuming $q=0$ and $\gamma_2=\gamma_3$ are independent of the direction of the magnetic field relative to the crystal axes. Corrections to the energies and wave functions arising from q and $\gamma_2-\gamma_3$ can be calculated by perturbation theory. With these corrections, the energies become dependent on the direction of the magnetic field. Each corrected wave function for $k_H=0$ now involves three or four Bloch functions rather than just two. When the spin-orbit splitting Δ is not large compared to the separation of the magnetic levels, as may occur in silicon for which Δ is 0.04 ev, then the wave function of any magnetic level of the valence band may involve linear combinations of all six $\varphi_M{}^{(J)}$ valence band Bloch functions. The presence of additional terms in the wave functions will make possible other IMO and CR transitions involving the valence band magnetic levels.

Thus far we have only considered the magnetic states for $k_H=0$. When k_H is not restricted to zero, the energies of the V_1 and V_2 magnetic states become complicated functions of k_H and each magnetic state forms a magnetic sub-band which may be expected to be parabolic only for small values of k_H. The curvature of the sub-bands will be determined by the constants γ_1, γ_2, γ_3, K and q which also determine the spacing of the magnetic levels for $k_H=0$. Furthermore, the wave functions for $k_H\neq0$ will involve additional terms not given in Eq. (27). These new terms can lead to additional optical transitions which, however, should not yield absorption peaks, since the matrix elements involved are proportional to k_H.

The solution of the set of two differential equations for the V_3 band yields simply

$$\psi_3{}^+ = G_l\varphi_{\frac{1}{2}}{}^{(\frac{1}{2})}, \quad \psi_3{}^- = G_l\varphi_{-\frac{1}{2}}{}^{(\frac{1}{2})}. \tag{28}$$

The corresponding energy eigenvalues $\epsilon_3{}^+(l)$ and $\epsilon_3{}^-(l)$ are characterized by only a single l and a single M, and have a uniform spacing between adjacent levels. Furthermore, since the V_3 band in Ge is a parabolic band, the magnetic states form simple parabolic magnetic sub-bands:

$$\epsilon_3{}^\pm(l,k_z) = \epsilon_3 - (\hbar^2 k_z{}^2/2m_3{}^*) - \hbar\omega_{03}(l+\tfrac{1}{2})\pm\tfrac{1}{2}g_3\beta H. \tag{29}$$

The g factor for holes in the V_3 band can also be expressed in terms of the "antisymmetric constant" K_3:
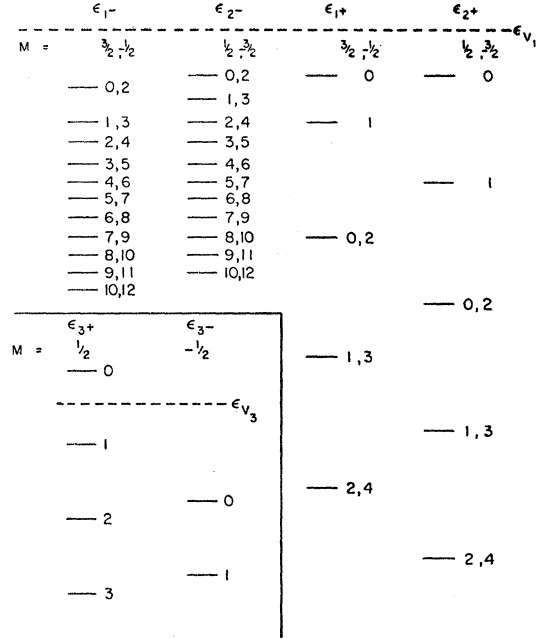
$$g_3 = 2(1-K_3). \tag{30}$$

FIG. 11. Energy levels of the V_1, V_2, and V_3 bands in Ge in the presence of a magnetic field. Numbers next to each level are the l values that characterize that level.

An estimate by Kohn, quoted by Luttinger,[20] leads to a value of -26 for K_3. This corresponds to a g factor of $+54$. Since the effective mass of holes in the V_3 band is $m_3{}^*=0.08m$, the separation $\Delta\epsilon$ between $\epsilon_3{}^+$ and $\epsilon_3{}^-$ sub-bands for the same l value is actually about two times greater than the separation between adjacent sub-bands in a given ladder. Furthermore, if the estimate of K_3 is accurate, the uppermost magnetic sub-band in the V_3 band, $\epsilon_3{}^+(l=0)$, will move closer to the V_1 and V_2 band edges, rather than away from them, as the magnetic field increases (Fig. 11).

B. Optical Transitions between the V_1, V_2, and V_3 Valence Bands and the Γ_2 Conduction Band in Ge

The Γ_2 band is spherically symmetric and has a two-fold spin degeneracy, but no orbital degeneracy. The wave functions to first order have the form

$$\psi^+ = G_l u_{\frac{1}{2}}{}^{(\frac{1}{2})}, \quad \psi^- = G_l u_{-\frac{1}{2}}{}^{(\frac{1}{2})}, \tag{31}$$

where we have designated the Bloch function by u to distinguish the conduction band Bloch function from the valence band Bloch function φ. For the Γ_2 conduction band which is S type in character, the Bloch functions $u_M{}^{(J)}$ can be written as

$$u_{\frac{1}{2}}{}^{(\frac{1}{2})} = S\alpha, \quad u_{-\frac{1}{2}}{}^{(\frac{1}{2})} = S\beta, \tag{32}$$

where S is a function which is totally symmetric with respect to the symmetry operations of the crystal. The energy levels of the magnetic states ϵ^+ and ϵ^- are
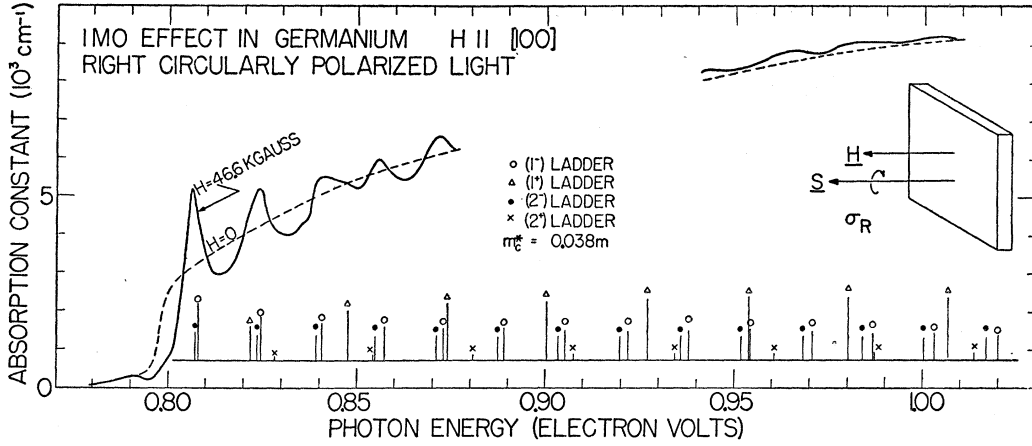
FIG. 12. Experimental absorption spectrum and theoretical absorption peaks for right circularly polarized light in Ge in a magnetic field at room temperature.

given by

$$\epsilon^{\pm} = \epsilon_0 + (\hbar^2 k_z^2/2m^*) + \hbar\omega_0(l+\tfrac{1}{2}) \pm \tfrac{1}{2}g\beta H. \quad (33)$$

Dresselhaus has estimated the effective mass of the electrons in the Γ_2 band to be $m^* \simeq 0.04m$. The last term in Eq. (33), which gives the separation of the magnetic levels of a given l arising from the interaction of the electron spin with the external magnetic field, may also be written as $\pm\beta H[1-K]$. The constant K is the antisymmetric constant for the Γ_2 conduction band. Roth[22] has derived the following theoretical expression for K using Kane's $\mathbf{k}\cdot\mathbf{p}$ perturbation method and considering only the interaction between the V_1, V_2, V_3 bands and the Γ_2 conduction bands:

$$K = [(m/m^*)-1][\Delta/(3\epsilon_G+2\Delta)], \quad (34)$$

where ϵ_G is the energy separation between the top of the valence band and the bottom of the Γ_2 conduction band. The value of K for Ge is calculated to be 2.5. The corresponding g factor is negative, $g \simeq -3$, so that the order of the sub-bands for the two spin states in a magnetic field is the reverse of that for an electron in free space.

Direct optical transitions from the V_1, V_2, and V_3 valence bands to the Γ_2 conduction band in Ge are allowed to first order in the absence of an external magnetic field. Corresponding transitions involving $\Delta l=0$ and $\Delta M=0$, ± 1 are therefore also allowed to first

TABLE I. Polarization properties for optical interband transitions.

n' \ n	1+, 1−		2+, 2−		3+, 3−	
	$\varphi_{\frac{3}{2}}^{(\frac{1}{2})}$	$\varphi_{-\frac{1}{2}}^{(\frac{1}{2})}$	$\varphi_{+\frac{1}{2}}^{(\frac{1}{2})}$	$\varphi_{-\frac{3}{2}}^{(\frac{1}{2})}$	$\varphi_{\frac{1}{2}}^{(\frac{1}{2})}$	$\varphi_{-\frac{1}{2}}^{(\frac{1}{2})}$
$u_{\frac{1}{2}}^{(\frac{1}{2})}$	σ_R	σ_L	π		π	σ_L
$u_{-\frac{1}{2}}^{(\frac{1}{2})}$		π	σ_R	σ_L	σ_R	π

order in the presence of an external magnetic field. Since a particular wave function in either the V_3 band or Γ_2 band involves only a single l and a single M value, the transitions between these bands yield terms in the matrix element similar to those that occur between simple energy bands. Consequently the σ_R and σ_L spectra will each consist of a single set of uniformly spaced peaks while the π spectrum will consist of a superposition of two sets of uniformly spaced peaks. The transitions between the V_1 and V_2 bands and the Γ_2 band, on the other hand, result in a greater number of terms in the matrix element and therefore yield a greater number of absorption peaks than occur for simple energy bands. This results from the fact that the wave functions of the V_1 and V_2 magnetic states are made up of the sum of two or more terms, each term involving a different (l,M) pair.

In applying the selection rule $\Delta l=0$, one must bear in mind that the l values involved are those appearing in the harmonic oscillator functions in the particular term of the matrix element under consideration.[23] The polarization effects associated with the individual terms in the matrix element are, on this basis, the same as those discussed for transitions between simple energy bands. Thus the $\Delta M=0$ terms in the matrix element correspond to π transitions which occur for plane polarized radiation with $S\perp H$ and $E\|H$; the $\Delta M=\pm 1$ terms correspond to σ transitions which occur for plane polarized radiation with $S\perp H$ and $E\perp H$ or for circularly polarized radiation with $S\|H$. The polarization properties of the absorbed radiation depend on which valence band functions $\varphi_M^{(J)}$ and conduction band functions $u_M^{(J)}$ are involved in the nonvanishing parts of the matrix elements. In Table I the polarization properties are summarized.

The transitions from the V_1 and V_2 bands to the Γ_2

[22] L. Roth, Lincoln Laboratory Solid State Research Quarterly Progress Report, November, 1957 (unpublished), p. 47.

[23] Since two values of l appear for each state, except for the upper two levels of the ϵ_1^+ and ϵ_2^+ level, the selection rule for n is $\Delta n=0$, ± 2.
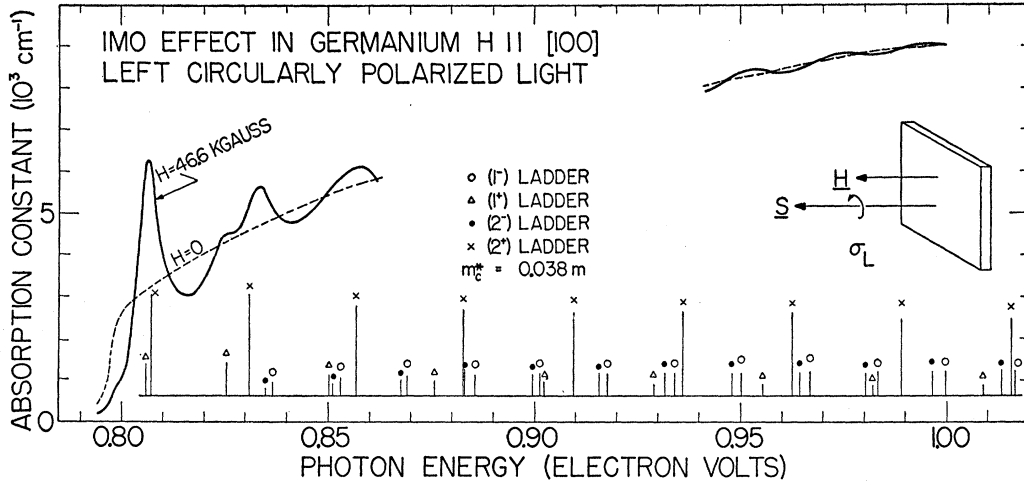
FIG. 13. Experimental absorption spectrum and theoretical absorption peaks for left circularly polarized light in Ge in a magnetic field at room temperature.

band yield 12 sets of absorption peaks, corresponding to one σ_L, one σ_R, and one π set for each of the four ladders. The transitions from the V_3 band to the Γ_2 band yield four sets of absorption peaks consisting of two π sets, one σ_R set, and one σ_L set.

The theoretical and experimental room-temperature IMO absorption spectra, together with theoretical positions of the absorption peaks for direct transitions between the V_1 and V_2 valence bands and the Γ_2 conduction band of Ge with the magnetic field directed along

[100], are plotted in Figs. 12, 13, 14, and 15 for right and left circular polarization with $S\|H$, and for $E\|H$ and $E\perp H$ plane-polarized radiation with $S\perp H$. The experimental curves were obtained from transmission measurements on a 3-micron-thick sample of Ge, made from material kindly supplied by C. Goldberg, Westinghouse Research Laboratories. A Perkin-Elmer grating spectrometer equipped with a 15 000-line/in. grating blazed at 1.6 microns, a tungsten light source, and a lead sulfide infrared detector were used in the measurements.
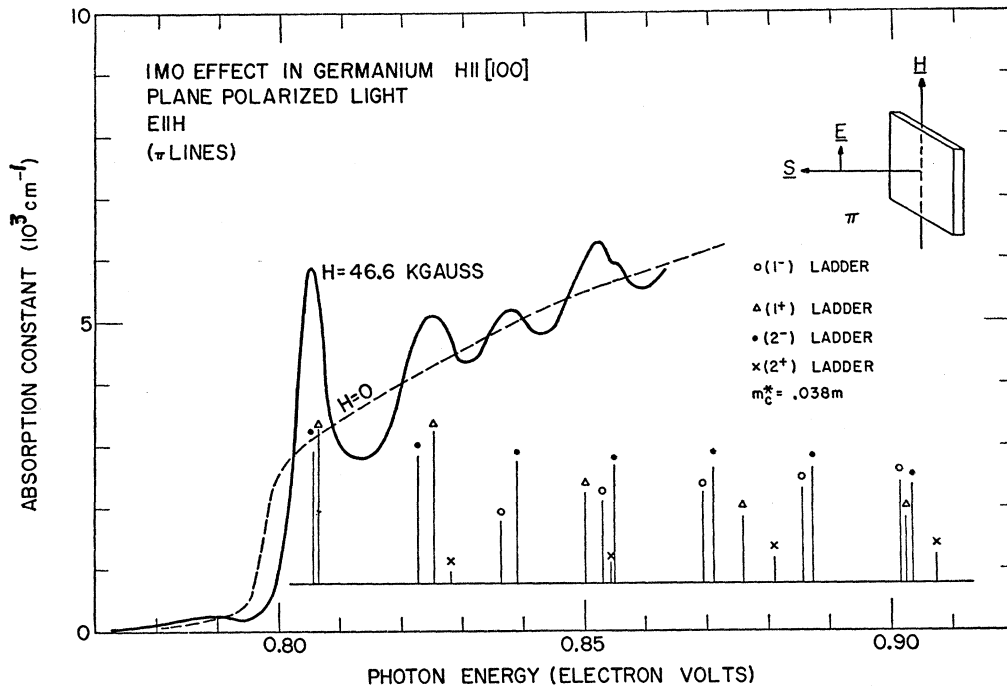

FIG. 14. Experimental absorption spectrum and theoretical absorption peaks for plane-polarized light with $E\|H$ in Ge in a magnetic field at room temperature. Beyond 0.94 ev the $H=0$ curve and high-field curves are coincident, as in the σ data in Fig. 15.
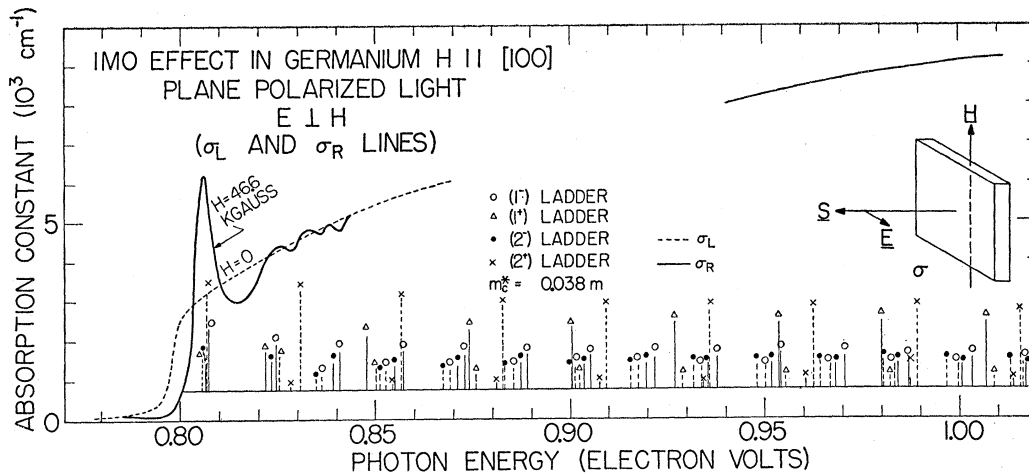
FIG. 15. Experimental absorption spectrum and theoretical absorption peaks for plane-polarized light with $E \perp H$ in Ge in a magnetic field at room temperature.

Infrared-transparent polaroid films were used to produce plane polarized light, and one such film together with a Fresnel rhomb made of NaCl was used to produce circularly polarized light. With no sample in place, a spectral band width of 10^{-4} ev could be resolved. With the sample in place, total energy transmitted is considerably reduced and the resolution in our experiments is about 5×10^{-4} ev. The spectrum between 0.86 ev and 0.94 ev was somewhat obscured by water bands and was therefore omitted from the curves.

The positions of the absorption peaks were calculated using values of the valence band energy levels kindly supplied to us by Goodman and Luttinger[24] together with Γ_2 conduction band energy levels calculated by assuming an effective mass of $0.038m$. This particular value of the Γ_2 conduction band mass gave the best match between theoretical lines and the experimental data in the σ_R spectrum. Although the assumption of uniform spacing of the magnetic sub-bands in the Γ_2 conduction band is not strictly valid because of nonparabolic effects, it is probably sufficiently accurate for the present data.

Relative theoretical values for the peak absorption coefficients given in Figs. 12–15 were calculated using approximate wave functions of Eqs. (27) and (31). The coefficients $a_1, \cdots b_2'$ appearing in the wave functions for the valence band levels were computed following the procedure of Luttinger,[20] using Goodman and Luttinger's values of the energy levels. The peak absorption coefficients were taken to be proportional to the square of the appropriate kinetic momentum matrix element. These matrix elements were all expressed in terms of a single momentum matrix element $(S|p_x|X)$ which was not further evaluated. We did not take into account the factor involving $\tilde{m}^*$ in the expression for the absorption coefficient. We also assumed that all IMO lines are characterized by the same broadening parameter.

Furthermore we did not attempt to plot a complete theoretical spectrum since this would have been a formidable task, and would involve questionable assumptions about the shape of the tails to the absorption peaks. Instead we have simply plotted the positions and relative heights of the peaks.

Although the individual peaks are not resolved in the experimental room-temperature spectrum, it is evident that there is reasonable agreement between the observed and theoretical positions of the absorption peaks. The width of the first absorption band in the π spectrum may be taken as a measure of the broadening of the individual peaks, since the separation of the two peaks which make up the band is small compared to the width of the band. It yields a value for $\Delta\epsilon$ of 2×10^{-3} ev in reasonable agreement with the value estimated from room-temperature lattice mobilities. It is possible to resolve additional structure by going to lower temperatures as has recently been demonstrated by the Lincoln Laboratory group in an experiment on Ge at liquid helium temperature.[6] The Lincoln Laboratory data lead to a value of $0.035m$ for the effective mass of the electron in the Γ_2 band.

It is of interest to note that the two unresolved peaks which make up the first absorption band in the room-temperature σ_L spectrum arise from the two uppermost levels in the light hole 1^+ and 2^+ ladders; in the case of the σ_R spectrum, they arise from the uppermost levels of the heavy hole 1^- and 2^- ladders; and in the case of the π spectrum, they arise from the uppermost levels in the 2^- and 1^+ ladders. The $S \perp H$ σ spectrum involves a superposition of the σ_L and σ_R absorption peaks, and is therefore a more difficult one to use in deriving information about the magnetic levels.

We also note that absorption peaks occur for higher l values in the $S \| H$ σ_R and σ_L spectra than in the $S \perp H$ σ and π spectra. This is believed to be due to the fact that for the $S \perp H$ configuration, in which the plane of the

[24] R. R. Goodman and J. M. Luttinger (private communication).

TABLE II. $\Delta l=\pm 1$ transition.

n \ n'	1+, 1-		2+, 2-	
	$\varphi_{-\frac{1}{2}}^{(\frac{1}{2})}$	$\varphi_{\frac{1}{2}}^{(\frac{1}{2})}$	$\varphi_{\frac{1}{2}}^{(\frac{1}{2})}$	$\varphi_{-\frac{1}{2}}^{(\frac{1}{2})}$
3+ $\varphi_{\frac{1}{2}}^{(\frac{1}{2})}$	$\pi(\Delta l=+1)$	$\pi(\Delta l=-1)$	$\sigma_L(\Delta l=+1)$ $\sigma_R(\Delta l=-1)$	$\sigma_R(\Delta l=+1)$
3- $\varphi_{-\frac{1}{2}}^{(\frac{1}{2})}$	$\sigma_L(\Delta l=+1)$ $\sigma_R(\Delta l=-1)$	$\sigma_L(\Delta l=-1)$	$\pi(\Delta l=-1)$	$\pi(\Delta l=+1)$

TABLE III. $\Delta l=0$ transition.

n \ n'	1+, 1-		2+, 2-	
	$\varphi_{-\frac{1}{2}}^{(\frac{1}{2})}$	$\varphi_{\frac{1}{2}}^{(\frac{1}{2})}$	$\varphi_{\frac{1}{2}}^{(\frac{1}{2})}$	$\varphi_{-\frac{1}{2}}^{(\frac{1}{2})}$
3+ $\varphi_{\frac{1}{2}}^{(\frac{1}{2})}$	σ_L	σ_R	π	$\cdots$
3- $\varphi_{-\frac{1}{2}}^{(\frac{1}{2})}$	π	$\cdots$	σ_L	σ_R

orbits is perpendicular to the plane of the sample, the interaction of the carriers with the surface increases with increasing orbit size leading to increasingly broadened absorption bands. For the $S\|H$ configuration, in which the plane of the orbits is parallel to the plane of the sample, the orbit size is negligible compared to the lateral dimension even at the highest l values involved.

Preliminary efforts to observe the IMO transitions between the V_3 band and the Γ_2 band at room temperature were unsuccessful. They are apparently masked by the transitions between the V_1 and V_2 bands and the Γ_2 band. Low temperatures, thinner specimens, and higher magnetic field may enable one to observe the V_3 to Γ_2 transitions.

C. Optical Transitions among the V_1, V_2, and V_3 Valence Bands in Ge

Although the V_1 and V_2 valence bands may be treated as separate bands in the absence of a magnetic field, it is no longer possible to do so in the presence of a magnetic field because of the quantum degeneracy effects discussed above. However, one can still associate the + and − ladders with light and heavy holes, respectively. Before discussing IMO type transitions between the magnetic levels of the valence bands, it may be of interest to point out that first-order CR type transitions involving $\Delta l=\pm 1$ and $\Delta M=0$, can take place between 1- and 1+ levels and between the 2- and 2+ levels, as well as between levels in the same ladder. This can be readily seen from an inspection of the wave function of the four ladders of magnetic levels of the V_1 and V_2 bands, if one remembers that CR transitions are those yielding nonvanishing terms in the matrix element which contain the same Bloch functions in the initial and the final state. The transitions between the + and − ladders may be looked upon as transitions between light-hole and heavy-hole bands. Since the initial state, with respect to hole transitions, is a heavy-hole sub-band and the final state is a light-hole sub-band, the CR transitions lead to absorption peaks with extended tails on the high-energy side, as in the case of IMO transitions, rather than to symmetrically broadened lines normally obtained for CR type transitions.[25] Furthermore, as pointed out by Kane,[26] the difference in spacing

---

[25] Transitions between sub-bands in the same ladder at low l values also lead to asymmetrically broadened lines because of the difference in curvatures of adjacent sub-bands.

[26] E. O. Kane (private communication).

of the + and − levels leads to CR absorption transitions which involve $\Delta l=-1$, as well as $\Delta l=+1$. These CR transitions therefore involve both right and left circularly polarized radiation, whereas CR absorption transitions of holes between levels in the same ladder take place only with right circularly polarized radiation. Additional CR type transitions may occur as a result of the presence of additional terms in the wave function when $\gamma_2\neq\gamma_3$. However, these transitions may be expected to be considerably weaker than the other transitions discussed above. CR transitions may also be expected to occur between levels in the $\epsilon_1^{\pm}$ and $\epsilon_2^{\pm}$ ladders, and those in the $\epsilon_3^{\pm}$ ladders in semiconductors where the spin-orbit splitting of the V_3 band from the V_1 and V_2 bands is small, so that the wave function of the magnetic levels of the valence bands involve linear combinations of all six $\varphi_M^{(J)}$ valence band Bloch functions.

As discussed in Sec. 2D, IMO type transitions between magnetic levels within the valence band (transitions yielding terms in the matrix element which contain the different Bloch functions in the initial or final state) can take place only to second order. Transitions that involve $\Delta l=\pm 1$, $\Delta M=0$, ± 1, ± 2 and $\Delta l+\Delta M=0$, ± 1 yield peaked absorption spectra, whereas transitions that involve $\Delta l=0$, and $\Delta M=0$, ± 1 yield nonpeaked absorption spectra.

The interband transitions from the magnetic levels of V_1 and V_2 bands to those of the V_3 band are of particular interest since for Ge they yield spectra which occur in an easily accessible region of wavelengths. Efforts to observe structure in the room-temperature V_1 and V_2 to V_3 IMO spectrum in p-type Ge have thus far been unsuccessful. The experiments are now being extended to low temperatures and to higher magnetic fields. A summary of the nonvanishing second-order transitions and the related polarization effects is given in Table II for $\Delta l=\pm 1$ and in Table III for $\Delta l=0$.

The curvatures of the 1- and 2- sub-bands are smaller than those of the 3+ and 3- sub-bands. The separations between them at $k_z=0$ are accordingly minimum separations. The corresponding $\Delta l=\pm 1$ spectra therefore exhibit long-wavelength limits, which occur at photon energies greater than Δ, the spin-orbit splitting, and which shift to higher photon energies with increasing magnetic field. Two $\sigma_L(\Delta l=+1)$ transitions from 2- to 3+ are exceptions to this in that they yield peaks at photon energies smaller than Δ, and shift to lower photon energies with increasing magnetic field.
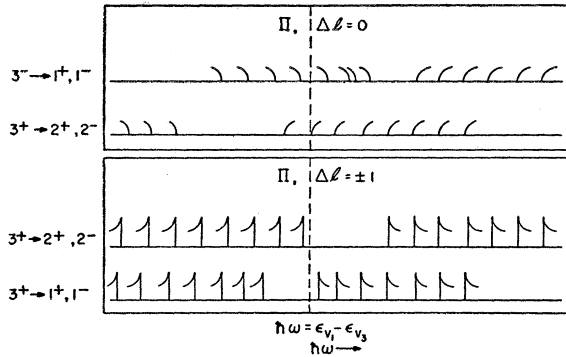
FIG. 16. Second-order IMO spectrum for transitions from V_1 and V_2 bands to the V_3 band in Ge in a magnetic field.

The 1^+ and 2^+ sub-bands have curvatures which are larger than those of the 3^+ and 3^- sub-bands. The separations between them at $k_z=0$ are accordingly maximum separations. The corresponding $\Delta l=\pm 1$ transitions exhibit short-wavelength limits, which occur at photon energies smaller than Δ and shift to lower photon energies. Two $\sigma_R(\Delta l=+1)$ transitions from 3^- to 1^+ and several $\sigma_L(\Delta l=-1)$ transitions from 3^- to 1^+ are exceptions, exhibiting short-wavelength limits which occur at photon energies larger than Δ and shift to higher photon energies. Similar effects also occur for the $\Delta l=0$, nonpeaked IMO spectra.

The positions and character of the π absorption edges for the $\Delta l=\pm 1$ and $\Delta l=0$ second-order IMO transitions from the V_1 and V_2 sub-bands to the V_3 sub-bands are shown schematically in Fig. 16. In the absence of experimental data for comparison, no effort was made to calculate the relative magnitudes of the free-carrier absorption constants which involve Boltzmann occupancy factors and are strongly temperature dependent. The vertical lines with tails extending to the right indicate ($\Delta l=\pm 1$) peaked absorption edges with tails extending to higher photon energies; the vertical lines with tails extending to the left are used to indicate $\Delta l=\pm 1$ peaked absorption edge with tails extending to lower photon energies; a line concave to the left indicates $\Delta l=0$ nonpeaked absorption edges with high photon energy limits; and a line concave to the right indicates $\Delta l=0$ nonpeaked absorption edges with low photon energy limits.‡

D. Optical Transitions between the Valence Band and Conduction Band in InSb

The calculations of the energies and the wave functions for the magnetic levels in the valence band of InSb

‡ *Note added in proof.*—A search for peaks in the intervalence band absorption of zinc-doped germanium in magnetic fields up to 58 000 gauss has been made by G. S. Picus and E. Palik at NRL. Runs were made at room temperature and at liquid nitrogen temperature with a sample containing 10^{15} zinc atoms per cm³, but no new peaks were observed at either temperature. A theoretical estimate indicates that the maximum intensities of the peaked transitions are no greater than those of the unpeaked transitions at a field of 60 000 gauss.

are similar to the calculations for Ge in their gross aspects, but differ in certain details. The principal difference between InSb and Ge is the absence of a center of symmetry in InSb. As a consequence, the V_1 and V_2 valence bands in InSb are not doubly degenerate bands at a given value of k except at $k=0$ [Fig. 10(b)]. The expressions of the energies for both bands in powers of k contain terms linear in k for certain directions in k space. The maxima of these bands accordingly do not occur at $\mathbf{k}=0$ as in Ge, nor do they coincide. The terms linear in k make the calculation of the magnetic levels of the valence band more complicated than for Ge, and at present such a calculation is not available.

In the case of the conduction band, the absence of a center of symmetry introduces cubic terms in k in the expression for the energy. The form of these cubic terms has been derived by Dresselhaus[19] who suggests that they are only important at values of energy comparable to or larger than the band gap. As pointed out by Kane,[27] the quartic terms in k which result from interaction between the conduction band and the valence bands are appreciable even at relatively low energies. These quartic terms in k lead to nonlinear separations between the magnetic sub-bands and result, for example, in an asymmetrical broadening of the CR absorption bands.[18]

The antisymmetric constant for the conduction band in InSb has a value of about 30 so that g is about -58. This rather large negative value for g, which was first pointed out by Roth,[22] results from the small effective mass of the electron, the large spin-orbit splitting Δ, and the small energy gap. The spin splitting of the conduction band magnetic level in InSb is accordingly quite large, being approximately one third the spacing between adjacent sub-bands in the same "ladder."

The IMO spectrum of InSb has been investigated at both NRL[3] and the Lincoln Laboratory.[4] A typical spectrum is shown in Fig. 17. Roth's suggestion that the separation between the first two bands corresponds largely to the separation between the conduction spin states for the $l=0$ level, appears to be a reasonable one. The separation between the first and third peaks appears to correspond to the separation between the $l=0$ and $l=1$ conduction sub-bands having $M_J=+\frac{1}{2}$. In the absence of an adequate theory of the magnetic levels in the valence band, further speculation about the interpretation of the IMO spectra is unwarranted at this time.

4. PRACTICAL CONSIDERATIONS

A. ω_0, τ Requirements

It is not possible to state, in any simple way, the ω_0 and τ requirements for observing well-defined absorption peaks in IMO spectra. Consider, for example, the IMO spectrum for allowed transitions between simple valence and conduction bands. The σ_R and σ_L ($S\|H$)

[27] E. O. Kane, J. Phys. Chem. Solids 1, 249 (1956).

spectra will each consist of only one set of uniformly spaced absorption peaks with a spacing equal to $\hbar\omega_{0n}+\hbar\omega_{0n'}$. A necessary condition for observing well-defined absorption peaks is that the spacing of the peaks be greater than the broadening of the peaks and therefore that $\hbar\omega_{0n}+\hbar\omega_{0n'}>\Delta\epsilon_n+\Delta\epsilon_{n'}=\Delta\epsilon_{nn'}$. This condition is obviously satisfied when both energy bands satisfy the condition $\omega_0\tau>1$, but it may also be satisfied when only one of the energy bands satisfies the condition $\omega_0\tau>1$ (Fig. 5). In the latter situation the width of the absorption peaks will be greater than the spacing of the sub-bands in the bands for which $\omega_0\tau<1$. However, even in this simple case the condition $\hbar\omega_{0n}+\hbar\omega_{0n'}>\Delta\epsilon_n+\Delta\epsilon_{n'}$, although necessary, is not sufficient for observing well-defined absorption peaks, because of the extended tails on the high-energy side of the absorption peaks of the individual sub-band-pair spectra. The existence of the extended absorption tails causes the absorption constant at successive peaks to increase, making it more difficult to resolve neighboring peaks. In addition the fractional contribution of the successive sub-band-pair spectra to the absorption constant decreases, making it succes-sively more difficult to observe the absorption peaks against the background absorption. The requirement for observing the absorption peaks in the corresponding π and σ ($S\perp H$) spectra are even more stringent than for the σ_R and σ_L spectra. The π and σ spectra each consists of two superimposed sets of peaks, the energy separation between the two sets being given by $|g_n\mp g_n|\beta H$, where the $-$ choice applies to the π spectra and the $+$ choice applies to the σ spectra. The necessary condition for resolving the two sets of peaks from one another in the π and σ spectra is $|g_n\mp g_{n'}|\beta H>\Delta\epsilon_n+\Delta\epsilon_{n'}$.

In the case of IMO transitions involving degenerate valence bands, the requirements for observing well-defined absorption peaks in the IMO spectra are even more complex. On the one hand, there are many more sets of peaks in a given spectrum, and on the other hand, the degeneracy effects in the valence band lead to an unequal spacing of the absorption peaks within a given set. Furthermore, the higher l-value peaks from different sets will move relative to one another as the magnetic field is varied and, at appropriate magnetic fields, levels for particular l values may actually coincide with one another. It is obviously not possible to make any precise statement regarding the $\omega_0\tau$ requirements for resolving the individual peaks. Nevertheless, the condition that $\hbar\omega_{0n}+\hbar\omega_{0n'}>\Delta\epsilon_n+\Delta\epsilon_{n'}$ is a useful criterion for deciding whether or not it should be possible to observe structure of any kind in first-order IMO spectra, as has been demonstrated in the case of Ge and InSb at room temperature.

The use of low temperatures to increase τ and therefore to decrease $\Delta\epsilon$, and the use of high magnetic fields to increase ω_0 should clearly be advantageous for observing detailed structure in the IMO spectra. The use of high magnetic fields will be particularly desirable in
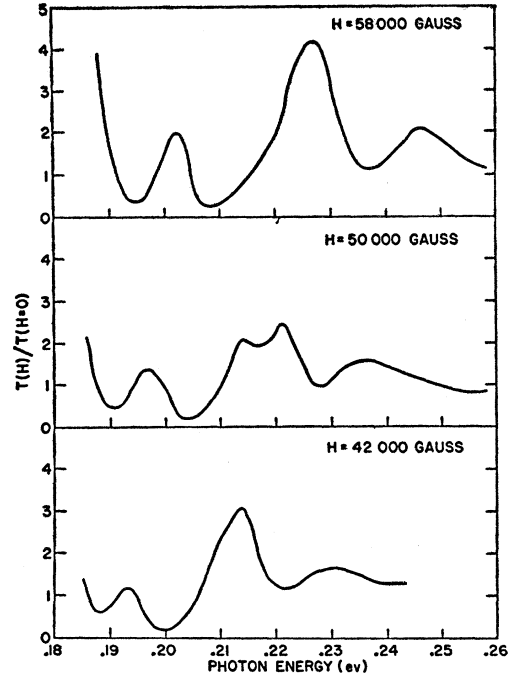

FIG. 17. Relative transmission, $T(H)/T(H=0)$, of InSb at room temperature plotted against photon energy at several magnetic fields [after E. Burstein and G. S. Picus, Phys. Rev. 105, 1123 (1957)].

the investigation of second-order IMO spectra in order to bring out the absorption peaks associated with the peaked $\Delta l=\pm 1$ transitions, since these are proportional to H^2, whereas the nonpeaked $\Delta l=0$ transitions are proportional to H.

B. Thickness Requirements

For a given $\Delta\epsilon_{nn'}$, there is a lower limit to the magnetic field, $H_{\min}$, above which it becomes possible to observe structure in the IMO spectrum. The magnitude of the absorption constant at the first absorption peak beyond the edge, and the experimental requirement that the product of the absorption constant and the thickness of the specimen be less than ~ 4.5 (optical density of ~ 2), further impose an upper limit to the thickness of the specimen, $d_{\max}\sim 4.5/A_1(H_{\min})$, where $A_1(H_{\min})$ is the absorption constant at the first peak. The latter can be taken to be approximately equal to the absorption constant at the corresponding position in the zero magnetic field absorption spectrum. For InSb and Ge at room temperature, $d_{\max}$ is of the order of 10 microns.

The use of magnetic fields larger than $H_{\min}$ for observing more detailed structure in the IMO spectra will obviously require the use of specimens with thicknesses appreciably smaller than $d_{\max}$. However, as the thickness of the specimen is decreased, one may encounter a situation in which $\Delta\epsilon$ is determined by surface effects rather than by bulk effects. In the $S\|H$ configuration, where the plane of the orbit is parallel to the plane of the

specimen, this will occur when the effective thickness of the specimen is comparable to or smaller than the mean free path between collisions. In the $S \perp H$ configuration, where the plane of the orbit is perpendicular to the plane of the sample, $\Delta\epsilon$ will presumably be determined by surface effects, when the orbit size becomes some appreciable fraction of the thickness of the specimen. Ideally, the effective thickness of the specimen would be equal to the geometrical thickness. In an actual specimen there may be an appreciable region close to the surface in which τ is much smaller than the bulk τ, so that the effective thickness will be smaller than the geometrical thickness. The relative importance of the surface region will obviously increase as the geometrical thickness decreases.

Because of the extended tails to the absorption peaks and the superposition of the bands it is not possible to give an explicit expression for the dependence of the peak absorption constants on $\Delta\epsilon$ and magnetic field, even in the case of simple energy bands. This, together with the lack of adequate theoretical or experimental information about the dependence of $\Delta\epsilon$ upon thickness, prevents one from giving a recipe for obtaining increased resolution in IMO spectra. In general, resolution will be favored by high magnetic fields, and the use of very thin specimens with a minimum of subsurface damage. With sufficiently high magnetic fields and appropriate specimen thickness, it should be possible in principle to obtain the necessary resolution even at room temperature. For magnetic fields limited to values below 60 000 gauss, greater resolution can be obtained by going to lower temperatures. This has been demonstrated by the Lincoln Laboratory group which has carried out measurements on a 3-micron-thick specimen of Ge at liquid helium temperature using plane-polarized radiation in the $S \perp H$ configuration. The decrease in band width of the peaks with decrease in temperature appeared to be smaller than that which would be predicted from the corresponding increase in the bulk τ. This is very likely attributed to the fact that the thickness of the specimen is comparable to the mean free path of the electron at low temperature. The use of the $S \perp H$ configuration may also be a contributing factor in causing a large $\Delta\epsilon$.

C. Instrumental Resolution Requirements

A reasonable requirement on the resolving power of optical instruments to be used in IMO experiments is that they be capable of resolving absorption bands whose separation is of the order of $\hbar\omega_0$ for carriers of effective mass $m^* = m$. Since observations are made at photon energies corresponding to the intrinsic band gap, the resolving power required is $\epsilon_G/\hbar\omega_0$. To get a numerical idea of what is required of the instrumentation it should be noted that, at a magnetic field of 30 000 gauss, $\hbar\omega_0$ for carriers with an effective mass $m^* = m$ is 3×10^{-4} ev. In wave numbers this corresponds to 2.8

cm^{-1}. A band gap of the order of 0.1 ev corresponds to a wave number of approximately 800 cm^{-1} (wavelength equal to 12 microns). Grating equipped infrared spectrometers capable of resolving 0.6 cm^{-1} at this wavelength are now commercially available.[28] These spectrometers will resolve approximately the same wave-number separation of bands throughout the whole infrared region from two microns to seventeen microns. Since resolving power in this region of the infrared is limited by available energy and poor detectors, it should be possible to improve this value by going to larger gratings and correspondingly larger optical systems, or to interferometers of the type recently developed by Strong and collaborators.[29]

In the visible and ultraviolet, where lack of energy generally no longer hampers optical work, it is the characteristics of the optical system itself which limit resolution. If one chooses diffraction gratings such that the grating space is approximately equal to the wavelength at which observations are to be made, then the minimum wave-number separation of bands which can be resolved is equal to the reciprocal of the width of the grating expressed in centimeters. If we make a fairly generous allowance for deviation of the grating from ideal behavior a resolution of 0.5 cm^{-1} can be obtained with a grating only five centimeters wide in a properly designed optical system.

D. Carrier Concentration Requirements

Cyclotron resonance requires the presence of free carriers. These may be generated thermally, optically, or by electrical breakdown. The carrier concentration must be small enough so that the cyclotron resonance frequency is greater than the plasma frequency, and yet must be large enough for reasonable specimen thickness to yield an observable cyclotron absorption band.

The IMO effect for intrinsic absorption processes does not depend on the presence of free carriers and therefore can be studied under conditions where, for well-defined cyclotron resonance experiments, the free-carrier concentration is either too small (as in materials with large energy gaps where it is not readily possible to generate free carriers) or too large (as in materials with small energy gaps where it is not possible to freeze out the carriers at impurity levels). It particularly lends itself to the investigation of the structure of energy bands whose extrema are away from the forbidden energy gap. In order to investigate such bands by cyclotron resonance, it would be necessary to generate carriers in the band by optical pumping. Attempts to carry out such investigations have been unsuccessful thus far, but should ultimately be possible in some materials.

Both cyclotron resonance and IMO effects can be

[28] R. C. Lord and T. K. McCubbin, J. Opt. Soc. Am. 45, 441 (1955); 47, 689 (1957).
[29] J. Strong, J. Opt. Soc. Am. 47, 354 (1957).

observed at room temperature, providing the conditions on $\omega_0\tau$, etc., are satisfied. However, in order to investigate quantum degeneracy effects by cyclotron resonance, it is necessary to go to sufficiently low temperatures so that only the lower l sub-bands are occupied. This has been accomplished thus far only for germanium by Fletcher et al.[30] who carried out microwave CR experiments at temperatures below 4°K. It should be possible to use appreciably higher temperature in CR experiments at infrared frequencies. Since the IMO effect does not depend on the distribution of free carriers in the magnetic sub-bands, it can be used to study quantum degeneracy effects without any restrictions on temperature other than those which arise from its effect on $\omega_0\tau$.

Both the IMO effect and CR yield information about the effective masses of the carriers and about quantum effects in degenerate energy bands. The IMO effect also yields information about the g factor for the carriers, and is useful for obtaining a precise value for the optical gap between the energy bands involved.

[30] Fletcher, Yager, and Merrit, Phys. Rev. 100, 747 (1955).

The IMO effect for transitions between two valence bands or two conduction bands does depend on the presence of carriers. Here, the absorption constants will generally be several orders of magnitude smaller so that it should be possible to use much larger specimen thicknesses.

5. ACKNOWLEDGMENTS

Specific Heat of Germanium and Silicon at Low Temperatures*

P. H. KEESOM AND G. SEIDEL†
Department of Physics, Purdue University, Lafayette, Indiana
(Received August 21, 1958)

The specific heats of several samples of silicon have been measured between 1.2°K and 4.2°K. The Debye characteristic temperature θ_0 at 0°K is estimated to be 636°K, a value slightly lower than previously reported. Measurements of germanium between 0.5°K and 4.2°K yield $\theta_0 = 363$°K, in very good agreement with older results.

From knowledge of the electronic specific heat and the carrier concentration of several degenerate samples of germanium and silicon, information is deduced concerning the energy band structure of the crystals. Measurements of n-type germanium indicate that the conduction band of this substance has four minima. Similar measurements of silicon indicate that there are six minima in its conduction band. The density-of-states effective masses of both electrons and holes in germanium, calculated from this work on degenerate samples, are not appreciably different than found from cyclotron resonance experiments on pure crystals. This result is consistent with the assumption, used in the calculations, that the addition of impurities to a crystal does not change the density of states in the vicinity of the band edge. For silicon, however, the specific heat yields somewhat larger effective masses for the electrons and holes than obtained from cyclotron resonance. Thus, the addition of impurities to silicon affects the shape of the bands.

INTRODUCTION

THE specific heats of the semiconductors silicon[1] and germanium[2] have previously been measured in the liquid helium temperature region. The present reinvestigations of these substances were primarily performed to obtain the electronic specific heats of both heavily doped n- and p-type germanium and silicon

samples. As is well known,[3] the specific heat of a degenerate electron gas is a direct measure of the density of states at the Fermi level. Then, by determining the specific heat and carrier concentration of a sample, it is possible to obtain information concerning the energy band structure of the crystal. By making certain assumptions regarding the energy dependence of the density of states, the effective masses of the carriers can be calculated for impure crystals. From measurements on n-type samples it is also possible to determine

[1] N. Pearlman and P. H. Keesom, Phys. Rev. 88, 398 (1952).
[2] P. H. Keesom and N. Pearlman, Phys. Rev. 91, 1347 (1953).
[3] F. Seitz, *Modern Theory of Solids* (McGraw-Hill Book Company, Inc., New York, 1940), p. 151.